https://doi.org/10.5194/egusphere-2026-4779
Preprint. Discussion started: 23 September 2026

Preservation of Glaciochemical Signals in a Warming Tropical Ice Cap: Evidence from the 2022 Quelccaya Ice Core

João Gomes Ilha[1,2], Manoela Brum Poitevin Portella[3,4], Oscar Vilca Gomez[5], Filipe Gaudie Lindau[3], Mariusz Potocki[6], Elena Barbaro[1,2], Susan Kaspari[4], Carlo Barbante[1,2], Jefferson Cardia Simões[3] and Paul Andrew Mayewski[6].

[1]Department of Environmental Sciences, Informatics and Statistics, Ca' Foscari University of Venice, Venice, Italy, 155 Via Torino, 30172 Venezia Mestre, Italy.
[2]CNR – Institute of Polar Sciences (ISP-CNR), 155 Via Torino, 30172 Venezia Mestre, Italy.
[3]Polar and Climate Center (CPC), Instituto de Geociências, Universidade Federal do Rio Grande do Sul (UFRGS), Av. Bento Gonçalves, 9500, 91501-970.
[4]Department of Geological Sciences, Central Washington University, Ellensburg, Washington, WA, 98926.
[5]Oficina Desconcentrada Macro Región Sur, Instituto Nacional de Investigación en Glaciares y Ecosistemas de Montaña (INAIGEM), Cusco, Peru.
[6]Climate Change Institute (CCI), University of Maine, Orono, ME, 04469-5790.

Correspondence to: João Gomes Ilha (joao.gomes.ilha@gmail.com)

Abstract. Paleoclimate records stored in ice cores are facing great threat as on-going mass loss is rapidly accelerating. To study Amazon's paleoclimate, an ice core was drilled in the Quelccaya ice cap, in Peru, in 2022. However, as a first step, post-depositional alterations need to be discussed and described. During drilling, one water table (WT) associated with the firn-ice transition and a major fracture at 45 m depth were identified. Here we present the first chemical results retrieved from the ice core and discuss the preservation state of the record in terms of post-depositional alterations. Concentrations of levoglucosan, Na^+, K^+, Cl^-, SO_4^{2-} and NO_3^- were analyzed and compared with the relatively insoluble and immobile black carbon signal. Furthermore, signal preservation was evaluated using descriptive statistics, covariance analysis, ionic balance, and multivariate classification. Statistical analyses reveal enhanced ion concentration atop the WT. The section below the WT extending to the fracture is marked by a highly altered chemical signal, as indicated by multivariate analysis. Within this interval, Cl^- is strongly depleted and Na^+ shows increased association with SO_4^{2-} and NO_3^-, while the ionic balance indicates increased acidity relative to the WT onset. Below the fracture, chemical signals are attenuated but largely preserved. Principal Component Analysis coupled to Fuzzy C-Means clustering independently identifies the WT, altered ice interval, the fracture zone and a deep ice anomaly, suggesting variable preservation along the core. We define depth intervals characterized by preserved, amplified, altered and attenuated signals and show that despite significant meltwater influence, post-depositional alterations are locally concentrated rather than affecting the entire record. These results provide a basis for future paleoclimatic investigations using what could be the last Quelccaya Ice Cap ice core before continued melting irreversibly alters the record.

Keywords: Quelccaya, ice core, glaciochemistry, paleoclimate, post-depositional processes, melting, Amazon.

1 Introduction

Deep ice cores have been used for the study of paleoclimatology, especially for the recent geological record (<1.2 Ma) and for the Holocene (Clifford et al., 2023; Dansgaard et al., 1969; Delmas et al., 1980; EPICA community members, 2004; Epstein et al., 1970; Gabrielli et al., 2016; Jouzel et al., 1982; Legrand et al., 1991; Mayewski et al., 1990; Schwikowski et al., 1999; Spagnesi et al., 2026; Thompson et al., 2013; Wolff et al., 2003; Xu et al., 2009). The

https://doi.org/10.5194/egusphere-2026-4779
Preprint. Discussion started: 23 September 2026

unparalleled time resolution that can be obtained from such climatic archives is of great importance, sometimes allowing for seasonal constraint of the record. Polar ice cores, mostly from the Antarctic and Arctic (Greenland), are the most studied and considered classical sites for ice core studies, revealing signals from seasons to millennia. Apart from the poles, glaciers and ice caps are also found in mountainous regions (e.g. Himalayas, Alps and Andes). Usually, studies in such places focus on the most recent record (Baccolo et al., 2026), the Holocene climate, pollution (Spagnesi et al., 2026), the anthropogenic signal (Legrand et al., 2025) and the rise and fall of civilizations (Thompson and Davis, 2014). Outside the poles, the Himalayas and Alps have been and continue to be vastly studied sites for ice core sciences. The Andes are also highly valuable for paleoclimatology, being one of the few mountain ranges outside the Antarctic to be glaciated in the Southern Hemisphere, however, even though it contains a larger volume of ice than the Alps, it has been less studied. A unique feature found in the Andes is the presence of large bodies of ice in tropical latitudes capable of recording with high resolution events that strongly impact present-day climate, such as El Niño Southern Oscillation (ENSO) and the South American Summer Monsoon (SASM) (Hurley et al., 2019; Thompson et al., 1984a, 2013, 2017; Vimeux et al., 2009).

In the recent decades, glaciochemistry has proven to be a reliable way to understand past climate. Accessing the climate records of tropical regions through ice cores is beneficial for understanding climatic teleconnections that operate in the region today. However, ice is being rapidly impacted by climate change, especially in the tropics (Lamantia et al., 2024; Salzmann et al., 2013; Vuille et al., 2008; Yarleque et al., 2018). Glaciers are facing ice loss, manifested primarily through melting and sublimation. These processes can provoke photochemical degradation of elements and elution through percolation of meltwater. A disturbed signal might lose its seasonality entirely or it might appear dislocated and smoothed, or it can even present enhanced concentrations of in-situ created species (Avak et al., 2018, 2019; Clifford et al., 2023; Eichler et al., 2001; Ginot et al., 2001; Thompson et al., 2011). The climatic record that was once reliably found in ice cores is being rapidly altered, leading to compromised chemical signatures, and in some cases the complete erasure with the disappearance of some glaciers.

The Quelccaya ice cap (QIC) is no different. Being a large body of ice positioned on the Cordillera Vilcanota in southeastern Peru at about 5674 m a.s.l. and abutting the Amazon basin, right on top of the Andean divide, it can record climatic processes from the region in high time resolution. Although few ice cores have been drilled in the region, the QIC has been intensely studied in recent decades, with the first two drilled on the summit in 1983 and 2003, by Thompson's team (Beal et al., 2014; Buffen et al., 2014; Clifford et al., 2023; Fritz et al., 2015; Hurley et al., 2019; Thompson et al., 1984a, b, 1985, 1986, 2011, 2013, 2017, 2021; Thompson and Davis, 2014; Thompson and Mosley-Thompson, 1987; Uglietti et al., 2015; Vuille et al., 2003; Weide et al., 2017).

Recent studies showed that the QIC might lose its accumulation zone entirely as soon as 2050 and completely disappear by 2100 (Yarleque et al., 2018). Because of its flat topography and negligible horizontal flow over the summit, the QIC is a good site to retrieve preserved and continuous paleoclimatic records. In 2022 a new ice core was drilled in the QIC. The 2022 QIC core has been analyzed at an unprecedented sampling resolution, and new techniques were applied to provide new chemical records for the region. As a first step, assessing the preservation of the chemical signal and the effect of post-depositional changes is of utmost importance. Temperate and tropical glaciers are facing a possible loss of their records in their entirety (Avak et al., 2018, 2019; Eichler et al., 2001; Ginot et al., 2001; Herreros et al., 2009; Hou and Qin, 2002; Thompson et al., 2011, 2017, 2021). In this study, we discuss the impact of post-depositional processes on the chemistry (soluble and insoluble) of the QIC and evaluate the preservation of the signal in it. We present the first chemical data of the 2022 Quelccaya ice core and use it to evaluate the preservation state of the glaciochemical archive,

https://doi.org/10.5194/egusphere-2026-4779
Preprint. Discussion started: 23 September 2026

identify depth intervals suitable for paleoclimatic analysis and propose a framework for assessing signal preservation in warming glacier archives. First, we present the most used markers of signal preservation and signal alteration, then we discuss their application in the QIC context and their relationship with the two features found during drilling: the water table and the fracture. Ion signals are then compared between each other through correlation schemes. The ionic balance is assessed, and multivariate techniques are used to cluster the signals and scan the ice core for altered chemistry. Depth intervals of identified and labeled according to their preservation state. This framework provides guidance for future studies using what could become the last Quelccaya deep ice core.

2 Materials and Methods

2.1 Study site

The ice core was drilled in a joint cooperation by the University of Maine (USA), the Universidade Federal do Rio Grande do Sul (Brazil) and the Instituto Nacional de Investigación en Glaciares y Ecosistemas de Montaña (INAIGEM, Peru) during the austral winter/dry season of 2022 in the summit of the QIC (13°55'46.099" S, 70°49'21.557" W, 5674 m a.s.l.) (Figure 1). Prior to the drilling, a geophysical survey that produced GPR transects of the ice cap, was conducted by the INAIGEM. The transects results were used to carefully select the best site for drilling. The drilling was performed with a thermal drill managed by the US Ice Drilling Program, and it reached bedrock at 128.54 m of depth after seven days of work. The temperature inside the borehole was 0 ° C. The bedrock at the summit is flat, as it is in most of the QIC (Thompson et al., 1985), and the base is cold; therefore, horizontal movement is negligible as most of the flow happens vertically, compressing the ice. As they were being retrieved, the ice sections were immediately processed (measured, described and tagged) and stored in high-density Styrofoam boxes that were kept buried in a snow trench. The first workday was conducted during the night to avoid photochemical reactions and the melting of the most superficial layers of firn. Important features noted during drilling include a water table (WT) at 18.99 m depth atop the firn-ice transition and a fracture that caused a drop of about 1 m in the drill at 45 m depth. The extent of the WT is not clear. It occurs in a firn context, filling the pores and forming a porous aquifer that probably stops existing at the pore close-off depth but that could continue as a fracture aquifer below that Having finished the drilling process, the boxes containing the ice sections were carried down the mountain to a freezer truck during the night to avoid temperatures that could damage the material and then put in a freezer container in a ship that took them to the Climate Change Institute (CCI) of the University of Maine where they were stored in freezers at -25 °C. During the transport the temperature was logged and no melting was recorded.

https://doi.org/10.5194/egusphere-2026-4779
Preprint. Discussion started: 23 September 2026

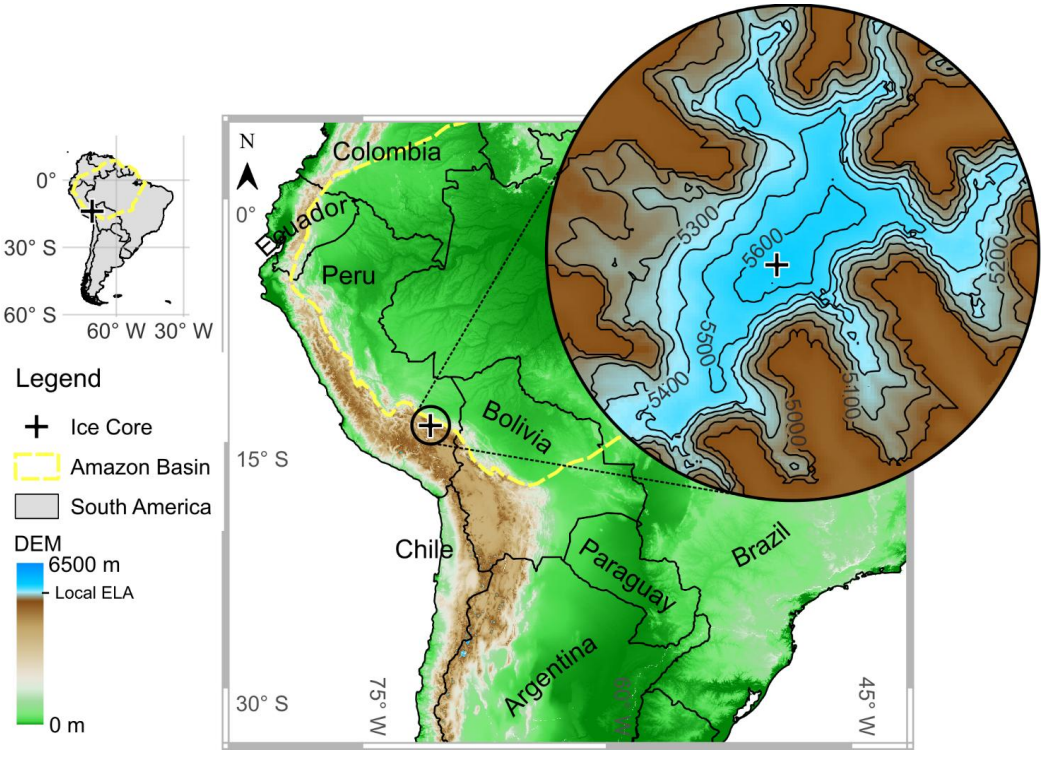

Figure 1: Map with the location of the 2022 Quelccaya ice core with a Digital Elevation Model (DEM) layer from Verdin (2017) showing the complex topography of the region and the areas above the local Equilibrium Altitude Line (ELA) from Lamantia et al. (2024) in blue. The Amazon basin limits are highlighted in yellow.

2.2 Pre-processing and subsampling

The ice core stored at the CCI was later sectioned in their ultra-cold laboratory (−25 ° C) using a stainless-steel-blade vertical bandsaw, periodically cleaned with methanol, and ice sections made of ultrapure water. The core was first cut in half to separate an archive section. The other half was then cut into three sections. The innermost section was selected for the analysis of dissolved impurities (described in this paper), major, trace, and rare-earth elements. The outer sections were dedicated to black carbon (BC), described in this paper, and microparticles. Additionally, parts of the archive section are being used for laser ablation (in progress). The innermost section was decontaminated by scrapping the surface of the ice under a laminar-flow hood using a ceramic knife. The decontaminated sections were then submitted to a subsampling process using a continuous-flow discrete-sampling (CFDS) framework (Osterberg et al., 2006) inside a clean room. The procedure sampled aliquots of the innermost section of 1.5 mL in pre-cleaned polypropylene vials. The subsampling yielded a resolution of around 2.0 cm per sample for depths from 0 to 20 m. Sampling resolution for the rest of the ice core was around 1.5 cm per sample. After the subsampling procedure, samples were stored at the CCI (USA) ultra-cold laboratory at −25 ° C for 2 months, and then they were shipped while frozen to the ultra-cold laboratory of the Institute of Polar Sciences of the National Research Council of Italy (CNR-ISP) where they were kept at −20 ° C until analysis.

The dissolved fraction was analyzed at CNR-ISP. Inorganic ions (Na^+, K^+, NH_4^+, Cl^-, Br^-, NO_3^-, Ca^{2+}, Mg^{2+}, SO_4^{2-}), methanesulfonic acid (MSA) and carboxylic acids (formic, acetic, glycolic, oxalic, malonic, succinic, glutaric, cis-maleic, trans-fumaric, adipic and pimelic) were analyzed using an ion chromatographer (Thermo Scientific Dionex™ ICS-

https://doi.org/10.5194/egusphere-2026-4779
Preprint. Discussion started: 23 September 2026

5000/6000, Waltham, MA, USA) coupled with a conductivity detection for cations and a single quadrupole mass spectrometer (MSQ Plus™, Thermo Scientific, Bremen, Germany) with an electrospray source (ESI) operating in negative mode (Barbaro et al., 2017, 2020) for anions. Levoglucosan samples were first spiked with an internal standard (20 µL of 25 µg L^{-1}) and then analyzed in a High Performance Liquid Chromatography (HPLC, Agilent 1100 series) coupled to a triple quadrupole mass spectrometer (API 4000) with negative ion electrospray ionization (Gambaro et al., 2008; Zennaro et al., 2014, 2015).

BC was analyzed at the Department of Geological Sciences, Central Washington University (CWU – WA, USA), where samples were prepared under a laminar-flow hood in a cold room by discrete sampling of 121 ice core sections, corresponding to 100.69 m. The sampling was performed by cutting the ice sections with a meat-grade stainless steel blade into smaller pieces (ice sticks). The ice sticks were then hand-scraped and cut, resulting in samples with sizes ranging from 2.0 to 2.5 cm, which were subsequently stored in 50 mL pre-cleaned polypropylene vials. Samples were kept frozen until just prior to analysis when they were melted at room temperature and sonicated for 15 minutes. BC analysis was conducted using an extended-range Single Particle Soot Photometer (SP2, Droplet Measurement Technologies, Boulder, CO, USA) coupled to a CETAC Marin-5 nebulizer, adopting the methodology presented by (Marquetto et al., 2020; Wendl et al., 2014). In the present work, we present data for selected ions, levoglucosan, and BC and discuss signal preservation.

2.3 Data Processing & Blanks

Raw ion chromatography data were retrieved and computed using Chromeleon v7.3. For levoglucosan the software used to retrieve and compute the data was Analyst v1.5.1. For BC the SP2 Toolkit version 4.200, developed by the Laboratory of Atmospheric Chemistry at the Paul Scherrer Institute (PSI), was used for data processing. All data were then processed and analyzed using different libraries in Python. The first set of blank samples (n=5) for dissolved species, called Field Blanks (FB) was collected prior to any melting in the CFDS and after 12 h of pumping of ultrapure water (MiliQ-Element >18.2 MΩ) through the system. Blanks for soluble species were also sampled every day prior to and after the melting of ice sections in the CFDS by pumping ultrapure water for 30 minutes and then collecting three samples (n = 164). For BC, procedural blanks made of Milli-Q water were measured prior to and after each working day and every 15 samples. The background levels were constantly below 0.01 µg L^{-1}. Concentrations were below the method detection limit (MDL) (Table S1); hence, no correction was made. Here concentrations of soluble analytes and BC are reported as nanomolar per liter (nmol L^{-1}) and microgram per liter (µg L^{-1}), respectively.

2.4 Descriptive Statistics, Signal Analysis & Multivariate Data Analysis

A framework of descriptive statistics, signal analysis and multivariate data analysis was applied to the analyte's depth profiles. The mean concentrations in nmol L^{-1}, the $\log_{10}$ of the variance in (LV) and a robust signal-to-noise ratio (SNR) were calculated. The LV is used to assess signal variability and dispersion and the SNR to evaluate signal peak intensity in comparison to the background. The LV is calculated using the variance pandas' function. It sums the squared deviations from the mean and then divides it by the number of samples minus 1 (Eq. (1)). The $\log_{10}$ of the results is calculated to

https://doi.org/10.5194/egusphere-2026-4779
Preprint. Discussion started: 23 September 2026

facilitate the interpretation. The SNR was applied by subtracting the median of the background concentration from the target value and then dividing it by the median absolute deviation (MAD) of the background (Eq. (2)).

$$LV = \frac{\sum(x_i - \bar{x})^2}{N-1} \quad (1)$$

$$SNR = \left(\frac{[analyte] - median_{background}}{MAD_{background}}\right) \quad (2)$$

The background was considered the zone with glacial ice, and where there was no interaction with the WT and the fracture (i.e. below 50 m). The purpose of the SNR was to verify concentration enhancement or collapse in the WT impacted zone; therefore, the background wasn't locally determined. The log-log regression was calculated using the HuberRegressor function from the scikit-learn's library and the Spearman correlations were calculated using the spearmanr function from the SciPy library. Spearman correlation was preferred instead of Pearson correlation because it is less sensitive to extreme spikes that are common in ice core records (e.g. fire plumes, volcanic eruptions, dust plumes). Spearman is also non-parametric, it doesn't require normally distributed data, and it evaluates monotonic, rather than linear relationships.

A Principal Component Analysis (PCA) is a multivariate statistical technique that transforms a dataset of correlated variables into a smaller dataset of principal components (PC). It evaluates the weights of the contribution of the variables that form the dataset. It is a powerful tool as it reduces the dimensionality of a dataset while retaining much of its variation. It does that by identifying the directions in which variables vary the most (Ringnér, 2008; Abdi and Williams, 2010; Shlens, 2014). The Fuzzy C-Means (FCM) is a clustering method that assigns each variable a degree of membership to every cluster. Unlike k-means, FCM allows samples to have partial membership in multiple clusters (Dunn, 1973; Bezdek, 1981). FCM analysis are useful for complex geochemical datasets (Bochang and Xuejing, 1985; Vriend et al., 1988; Meng et al., 2011; Fatehi and Asadi, 2017), such as ice cores, because samples can represent multiple processes, which would be overlooked by a hard clustering method. The multivariate data analysis was performed by applying a PCA and an FCM in combination to identify groups of signals relevant to the present work. Both analyses were performed in Python (Ilha, 2026). The PCA was calculated using the scikit-learn library. The data were standardized using scikit-learn's StandardScaler preprocessing method. Three principal components were retained based on the scree plot and the eigen values. Varimax rotation was applied using the Rotator function within the framework of the factor_analyzer library. The Kaiser-Meyer-Olkin (KMO) test and Bartlett's test of sphericity were computed using the same library to assess the suitability of the dataset for PCA analysis. FCM was performed using the fuzz function of the scikit-fuzzy library. The number of clusters was set to three, and the fuzziness parameter was set to two.

3 Results & Discussion

As a first step, we assess the concentration profiles for ions, levoglucosan and BC with depth, and the WT level, shown in Figure 2. All species show variation in concentration with depth, indicating at least a partially maintained natural variability, i.e., a partially preserved signal. Their signals are therefore not completely erased. It is also observable that Na^+, K^+, Cl^-, SO_4^{2-} and levoglucosan show increased concentration right on top of the WT. Below the fracture at 45 m depth, all species, except for BC, which is insoluble, show an attenuated signal in the mid-depth ice core (50 to 100 m depth). Nevertheless, variability is still preserved, as inferred from peaks increasing above the background, suggesting that the soluble chemistry signal is not completely homogenized despite meltwater redistribution.

https://doi.org/10.5194/egusphere-2026-4779
Preprint. Discussion started: 23 September 2026

200 BC depth profile shows strong seasonality, with peaks in the dry season, and valleys in the wet season, in agreement with what was discussed in Osmont et al. (2019) and Gilardoni et al. (2022) for nearby sites in the Andes. Peaks and valleys are constant, and they show a thinning with depth, typical of the compaction of the ice. Also, at first glance, BC signal doesn't seem to be affected either by the WT, nor by the fracture. Such results suggest that the BC could be a valuable indicator of preserved seasonality in the ice core. In the next section, we further discuss its signal and application in the
205 QIC context.

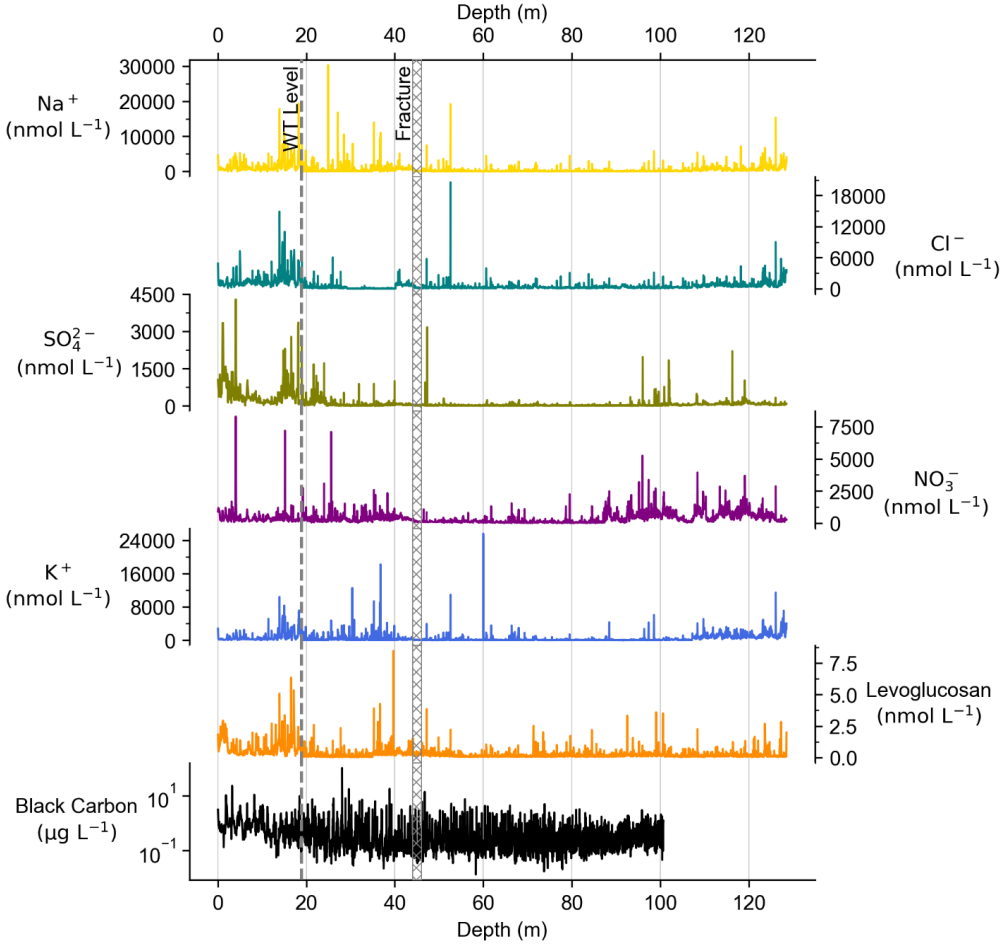

Figure 2: Concentration of Na^+, Cl^-, SO_4^{2-}, NO_3^-, K^+, levoglucosan in nmol L^{-1} and black carbon in µg L^{-1} with depth (in meters) for the 2022 Quelccaya ice core. The gray dashed line marks the WT level and the hatched area the fracture zone.

3.1 Common Markers of Signal Preservation & Signal Alteration

210 To evaluate whether signal is preserved or altered, we use some chemical markers. Black carbon, for example, is an insoluble and highly hydrophobic particulate (Wendl et al., 2014). It is generally preserved and regarded as a relatively immobile species. To check for the stability of BC signal in the 2022 Quelccaya ice core, we calculated the LV and SNR

https://doi.org/10.5194/egusphere-2026-4779
Preprint. Discussion started: 23 September 2026

in the zones that are interacting with the WT (depth intervals 10–20 m and 20–30 m) and with the fracture (depth intervals 30–40 m and 40–50 m). Results suggest that signal is preserved and highly variable. An average LV=4.23 indicates data variation and an average SNR=6.02 suggests that peaks rise above background, marking depositional events (Supplementary Table 1). These results converge with the hypothesis that BC signal variation is preserved with peaks that rise above the background level. Such characteristics reinforce the use of BC signal to constrain preservation and mobilization of other markers. Hence, it is here considered a local marker of signal preservation.

A marker that can be used to assess alteration of signal, especially because of the WT impact in the ice core, is the Cl^-/Na^+ ratio that indicates a deviation from the natural sea spray signature (here considered as close to 1.17 (Finlayson-Pitts and Pitts Jr., 1999), using a molar ratio). It is commonly used and could either reveal a Cl^- depletion, which is common in long-distance transport through the volatilization of Cl^- to form HCl (Xu et al., 2013), or a Cl^- enrichment that could be related to elution processes breaking the NaCl molecule (Eichler et al., 2001; Moser et al., 2024). An enrichment could also be derived from transport influx of Cl^- due to biomass burning, especially in the fine-mode aerosol, related to mid- to long-range transport (Liu et al., 2022).

3.2 BC and Cl^-/Na^+ in the Quelccaya Context

In this section we discuss the use of BC and Cl^-/Na^+ in the specific context of the QIC, and we apply it in the zone where there is interaction with the WT. The QIC is in a unique geographical position, receiving most of its precipitation from the east, with mixed signals that come from the Atlantic Ocean and the Amazon rainforest (Hurley et al., 2015; Thompson et al., 2013, 2017). Therefore, it is too simplistic to say that Cl^- and Na^+ are mostly due to sea salt aerosols. Apart from the impact that the Amazon rainforest atmosphere has on the aerosols that end up being transported to the QIC (Artaxo et al., 2013; Jardine et al., 2015; Ramsay et al., 2020), many local ecosystems (e.g. freshwater lakes, ultra saline lakes, salt deposits, and local dust with hyper arid and acid compositions) might also influence the composition of the ice core (Fritz et al., 2015; Pueyo et al., 2021; Weide et al., 2017). Deep convection is also expected and has already been described for the Illimani ice core (Lindau et al., 2021), which is located in a similar regional context to the QIC. This means that the contribution of local sources to the aerosol composition over the QIC should not be negligible, as supported by Clifford et al. (2023), Fritz et al. (2015), and Weide et al. (2017). Therefore, we opt not to use Cl^-/Na^+ as an unequivocal proxy for melt-affected ice; instead, we evaluate it alongside other chemical species and statistical and multivariate evidence.

A zoomed-in plot of the concentration of BC on a logarithmic scale with target depth intervals, which correspond to the section of the ice core that could be affected by the WT (from 10 to 50 m), is shown together with Na^+, Cl^- and Cl^-/Na^+ in Figure 3. BC shows seasonal-scale variation and preserved peaks below the depth where the WT level was observed, as well as above it. We consider, thus, that the BC signal is relatively immobile in the QIC ice core and that it can be used to constrain other soluble species' behaviors. The Cl^-/Na^+ ratio is low in the superficial layers (above the WT), but it increases right below the top of the WT at around 19 m depth down to around 25 m depth, indicating a possible altered zone where elution removed Na^+ faster than Cl^-.

https://doi.org/10.5194/egusphere-2026-4779
Preprint. Discussion started: 23 September 2026

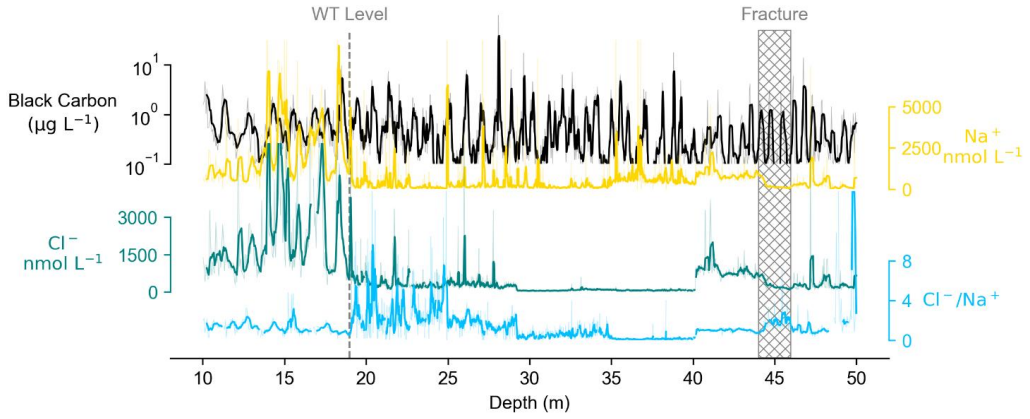

Figure 3: Preserved intensity and seasonality in the black carbon, Na^+, Cl^- and Cl^-/Na^+ record between 10 and 50 m. The vertical gray line indicates the level of the identified water table, and the hatched area indicates the fracture zone.

Below 25 m, Cl^-/Na^+ values drop and vary close to the sea spray ratio. In the fracture zone, the values increase weakly. Below that, Cl^-/Na^+ shows some spikes consistently down to 70 m depth (Figure 4). During drilling, no water table was identified at this depth. If the Cl^- enrichment at this depth interval is not related to elution, then it should be related either to enrichment from long-range transport, possibly due to Amazonia's atmospheric interactions, or local source aerosols, as discussed in the next section.

3.3 Markers of Signal Preservation & Alteration Below the Water Table

After having constrained the behavior of BC and Cl^-/Na^+ in depth intervals that interact with the WT, it is necessary to evaluate them for depths below the WT, as discussed next. In Figure 4, depth profiles of levoglucosan and NH_4^+ are compared with Cl^-/Na^+ and BC. Levoglucosan is in very low-concentrations and is primarily an indicator of biomass burning events. NH_4^+ is an indicator of biomass production and biomass burning events. Comparing both signals to the Cl^-/Na^+ signal, it's possible to see that when levoglucosan spikes, NH_4^+ usually also spikes, suggesting a possible signature of Amazonia's wildfires (#1 in Figure 4). Such behavior is not followed by Cl^- enrichment. Therefore, in this case the Cl^- enrichment is not tied to long-range transport. Some spikes of NH_4^+, however, are not followed by levoglucosan (#2 in Figure 4) but are by Cl^- enrichment. This could indicate that NH_4^+ may be related to local sources, meaning that some peaks of Cl^- enrichment can be produced by local geochemistry, as in the hyperarid environments of the Central Andes (Pfeiffer et al., 2019). Other peaks of Cl^- enrichment are not linked to NH_4^+ (#3 in Figure 4), which could be an indication of locally altered ice due to elution. If that is the case, the alterations seem to be restricted to small layers, not significantly affecting the ice core's signal.

https://doi.org/10.5194/egusphere-2026-4779
Preprint. Discussion started: 23 September 2026

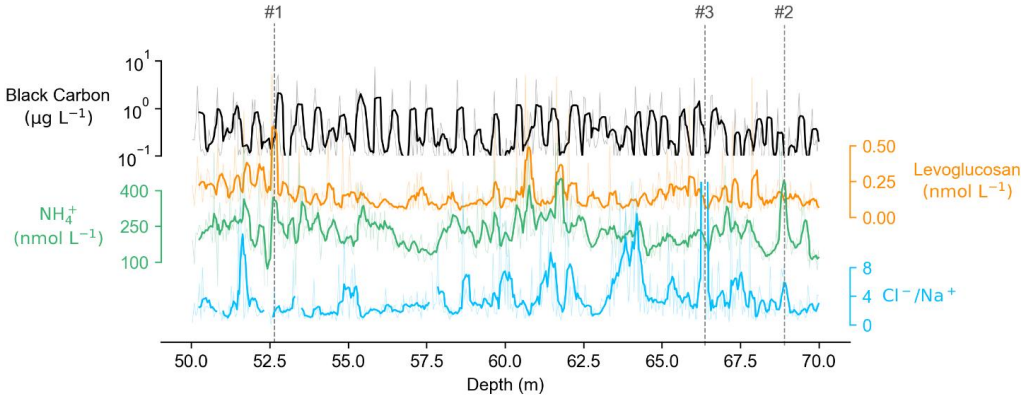

Figure 4: BC, levoglucosan, NH_4^+ and Cl^-/Na^+ signals below the fracture zone.

3.4 Ion Signals and the Water Table

BC and Cl^-/Na^+ are described both in regards with the WT and below it. These two markers assist the discussion of whether ion signals are preserved or altered. This section concentrates on the discussion of ions signals in depth intervals interacting with the WT, using the chemical markers are guides. To assess the behavior of ion signals with depth, we calculate the mean concentration, the LV and the SNR and display the results of selected ions in Table 1. Na^+, Cl^- and SO_4^{2-} have higher concentrations in the superficial layers, from 0 to 20 m depth, compared with their signal in the rest of the ice core. The concentration, LV and SNR of these species increase drastically right above WT. For instance, in the depth window from 10 to 20 m, Na^+ shows a 74 % concentration increase, variance spikes by 5-fold, and SNR goes up approximately 79% compared to the previous section (0–10 m). For the same interval, Cl^- shows a concentration increase of 48 %, a 4-fold higher variance, and an SNR that spikes 57 % higher. SO_4^{2-}, on the other hand, shows a decrease in concentration of 40.5 %, 1.62 times lower variance, and an SNR 42 % smaller. These results indicate a mobility of Na^+, Cl^- and SO_4^{2-} within the firn pack. The percolation and flux of meltwater in the superficial porous layer facilitates the transport of such ions, concentrating them right on top of WT. Although SO_4^{2-} shows different statistical results compared to Na^+ and Cl^-, these are probably influenced by the very high concentration of sulfate in the first 4 m of firn that masks the increase in concentration that happens above WT. The high concentration of sulfates in the first meters could be of volcanic origin caused by the eruption phase (volcanic explosivity index of 3) that happened between 2016 and 2020 in the Sabancaya volcano (15°47'26.5776" S; 71°51'17.1684" W), approximately 200 km distant from the QIC (Global Volcanism Program | Sabancaya, 2026). This activity produced up to 7000 tons per day of SO_2 with ash plumes as high as 5000 m above the crater (Coppola et al., 2022). However, it could also have an anthropogenic origin or even a biomass burning origin. If it was of anthropogenic origin, an increase in NO_3^- would also be expected, but such an increase does not occur as widely, only in some thin, sharp peaks. Levoglucosan, however, has high concentrations in the first meters, strengthening the biomass burning origin hypothesis. A concentration increase of levoglucosan doesn't follow sulfate below 2.5 m depth, suggesting that SO_4^{2-} is probably a mix of volcanic and biomass burning aerosols.

The signal over the WT is amplified (Figure 5) by the accumulation of ions transported through the firn pack; however, variability is maintained. Right below the WT level (20 to 30 m depth), this behavior changes. Na^+ concentration decreases by 81 % with a 2.6 times loss of variance and 84 % of SNR reduction in comparison to the 10 to 20 m depth interval. Cl^- follows the trend of decreasing concentration with a reduction of 83 %, 21.9 times lower variance and 94 % drop in SNR for the same depth interval. SO_4^{2-} has a decrease in concentration of 59 % with 5.37 times lower variance and 61.5 %

https://doi.org/10.5194/egusphere-2026-4779
Preprint. Discussion started: 23 September 2026

smaller SNR. This behavior is consistent with a probable elution process in the WT and at the beginning of the ice section. Concentrations are attenuated but variance and SNR are still considerably high (SNR Na^+: 6.12 and SO_4^{2-}: 16.98, less so for Cl^-: 1.29) indicating that the signal is attenuated but still preserved in this region and that Cl^- appears to be the strongest affected ion.

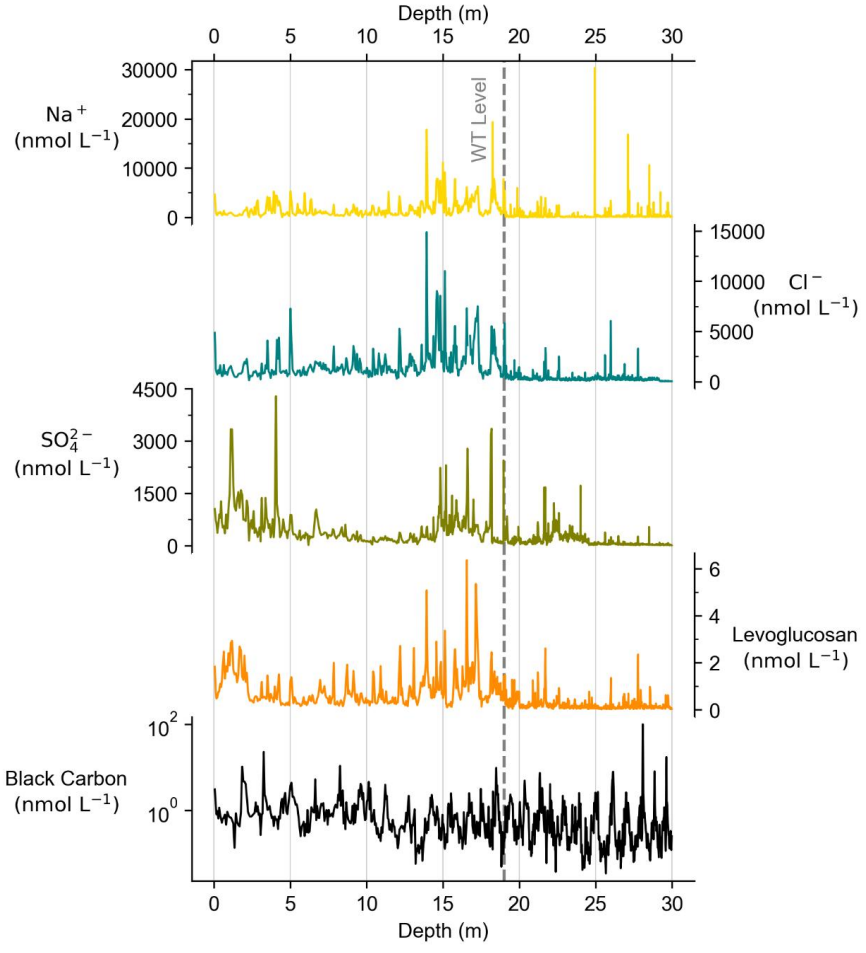

Figure 5: Detailed depth profile of selected species. The gray dashed line indicates the WT level.

3.5 Ion Signals and the Fracture

Similarly to what was discussed in the previous section, the assessment of how ions behave regarding the fracture is important to understand the pathways of alteration in the 2022 Quelccaya ice core. The fracture zone also seems to affect some of the ion signals, although differently than the WT. From 30 to 40 m the signal is slightly dampened for most but not all ions (Table 1). Na^+ maintains high variance, 2.75 times lower than previously but with an SNR ratio of 8.81, which is consistent with a preserved signal. Cl^- loses seasonality and is highly affected. Cl^- variance drops almost 155-fold and SNR drops by 244 %. SO_4^{2-} is also very impacted, although less so than Cl^-. Variance decreases 8.3 times and SNR by

https://doi.org/10.5194/egusphere-2026-4779
Preprint. Discussion started: 23 September 2026

83 %. For the rest of the ice core, Na^+ maintains signal characteristics that indicate an attenuation of intensity but preservation of variability, based on high variance and SNR. Na^+ SNR tends to decrease with depth, probably by diffusion, until approximately 100 m down, from which concentration, variance and SNR increase exponentially to the bedrock. Cl^- also maintains its signal throughout the ice core with the same tendency to dampen with depth but to enrich in the deep ice. SO_4^{2-} on the other hand seems to be more affected by the dampening of signal below the facture zone, showing considerable decrease of SNR (minimum of 0.15 at depth 80–90 m). Despite the intense attenuation of the signal, SO_4^{2-} appears to be preserved enough so that large deposition events are identifiable. Variability is still seen (although it loses power). The most intense peaks, probably the result of volcanic events, such as the Huyanaputina of 1600 CE, are sharp and well represented. Almost all species are enriched in the deep ice. There are many scenarios that could explain such behavior; inputs from bedrock, drastically different climatic conditions or even sample resolution effects. The deep ice layers of the QIC core are likely strongly compressed (Clifford et al., 2023) which could affect the identification of annual layers at the resolution reported in this study. Because of this, deep ice will be further investigated and discussed in a future paper using ultra-high-resolution techniques.

Table 1: Mean concentrations in nmol L^{-1}, log_{10} of variance (LV) in $nmol^2.L^{-2}$ and signal-to-noise ratio (SNR) of Na^+, Cl^- and SO_4^{2-} for 10 m depth windows for the 2022 Quelccaya ice core. Bold values indicate the depths within WT effect range.

Depth Interval (m)	Na^+			Cl^-			SO_4^{2-}		
	Mean	LV	SNR	Mean	LV	SNR	Mean	LV	SNR
0–10	1155.73	6.09	21.32	1305.97	5.93	13.62	567.13	5.51	75.64
10–20	2017.41	6.79	33.34	1929.96	6.58	21.39	337.3	5.29	44.12
20–30	**383.14**	**6.37**	**6.12**	**315.86**	**5.24**	**1.29**	**139.45**	**4.56**	**16.98**
30–40	**522.75**	**5.93**	**8.82**	**62.84**	**3.05**	**-1.86**	**36.94**	**3.64**	**2.92**
40–50	**560.66**	**5.70**	**9.56**	**538.08**	**5.53**	**4.06**	**56.57**	**4.62**	**5.61**
50–60	267.76	6.22	3.78	368.24	6.26	1.94	21.93	2.81	0.86
60–70	215.64	5.36	2.75	319.646	5.14	1.34	27.38	3.11	1.61
70–80	210.91	5.30	2.66	305.94	5.09	1.17	21.85	2.68	0.84
80–90	164.35	5.09	1.74	301.93	4.97	1.12	16.81	2.42	0.15
90–100	154.86	5.32	1.55	313.59	4.89	1.26	44.74	4.36	3.99
100–110	403.68	5.59	6.46	407.75	5.09	2.44	78.62	4.40	8.63
110–120	743.46	5.67	13.17	735.60	5.23	6.52	111.975	4.44	13.21
120–130	1288.18	6.39	23.94	1217.16	6.10	12.51	76.84	3.22	8.39

Most of the works describing elution in glaciers points out that Cl^- behaves similarly to Na^+ and is generally the least mobile of major ions (Avak et al., 2019; Brimblecombe et al., 1987; Davies et al., 1982; Davis et al., 1995; Eichler et al., 2001; Herreros et al., 2009; Rempel et al., 2001), while SO_4^{2-} is, in most cases, the most prone to elute. However, in some depths of this core Cl^- is more strongly affected by post-depositional processes than the other ions. This behavior could be due to the bonds that Cl^- forms, as discussed in (Ginot et al., 2001); Cl^- bonded to Na^+ to form salts is more stable than when bonded to H^+ to form HCl. The preservation of the Cl^- signal seems to vary along the ice core. Perhaps, the cations to which it is bonded also change. This problem is discussed in the next section.

https://doi.org/10.5194/egusphere-2026-4779
Preprint. Discussion started: 23 September 2026

3.6 Ions Correlation

Ions behave in combination with each other. Cations and anions bond to form molecules. However, the stability of such molecules is highly dependent on the environment. After having described how ions vary in depth and in comparison to the chemical markers, we focus on describing and discussing how ions interact with each other. Such correlations can suggest recombination of ions in depth due to environment forcing. Na^+ and Cl^- usually strongly co-vary due to the large influence of sea salt aerosols on the chemistry of ice cores and also the high probability of NaCl salt forming (Legrand and Mayewski, 1997). However, the QIC is surrounded by many dichotomically different ecosystems that can be source areas for ions forming different molecules (e.g. the Amazon rainforest, the ultra-saline lakes of the Altiplano-Puna plateau, and oceans). In order to evaluate the behavior of the sodium-chloride system, we calculated the log-log regression and the Spearman correlation (denoted as ρ) between both variables. Since the extension of the WT and its impact on the ice core is not clear, we performed exploratory calculations using fixed 10 m depth windows, shown in Table 2, as well as for the whole ice core as one. We present the results for the ice core in its entirety (Figure 6) and for the first 40 m using the fixed 10 m depth windows (Figure 7 7). Sodium and chloride show strong correlation for most of the ice core (Table 2, Figure 6). However, it is noteworthy to add that the correlation between the two species varies in depth. At shallow depths (< 10 m) it is moderate ($\rho = 0.41$) with an increase until depths of 20 m ($\rho = 0.876$) (Figure 7(a) and (b)) and a strong decoupling from 30 to 40 m ($\rho = -0.035$) represented by the blue-colored clusters in Figure 6 and shown in detail in Figure 7 (d). Below 40 m depth, correlation gets strong to very strong ($0.7 < \rho < 0.92$) down to 128.5 m, except from 90 to 100 m and from 110 to 120 m where correlation drops to moderate values ($\rho = 0.444$ and $\rho = 0.439$, respectively) (Table 2).

Table 2: Spearman correlation between Na^+ and Cl^- in 10 m depth windows.

Depth Intervals (m)	ρ
0–10	0.411
10–20	0.876
20–30	0.469
30–40	−0.035
40–50	0.916
50–60	0.788
60–70	0.705
70–80	0.756
80–90	0.752
90–100	0.443
100–110	0.736
110–120	0.445
120–128.5	0.830

https://doi.org/10.5194/egusphere-2026-4779
Preprint. Discussion started: 23 September 2026

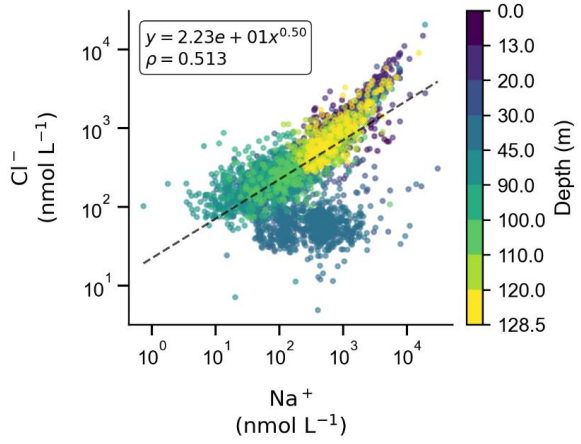

Figure 6: Log-log regression between Na^+ and Cl^- concentrations color coded by depth. The dashed black line is the robust regression line calculated using the HuberRegressor function of the sci-kit library of Python.

The generally slightly faster elution of Na^+ over Cl^- happens mostly due to these elements positions in the ice (Avak et al., 2019; Bohleber et al., 2025; Cragin et al., 1993; Eichler et al., 2001; Stoll et al., 2021; Trachsel et al., 2019). Na^+ is often positioned at grain boundaries and is more readily available for transport with meltwater percolation than Cl^-, which occupies inner positions on the ice grains. However, Cl^- is also regarded as suffering more from diffusion in consolidated ice, as in the mid- and deep ice, because it is easily transported in the very fine grain limits due to its smaller size compared to Na^+. In the QIC case, Cl^- seems to be more affected by post-depositional processes than Na^+ in some parts of the ice core. This behavior is highlighted between 30 and 40 m depth, as indicated by the strong decoupling seen in the correlation plots with Na^+, as depicted in Figure 6 and Figure 7, the 155-fold drop in LV, and the SNR of −1.86, as shown in Table 1. Elution sequences are tricky to identify in complex environments without very specific elution experiments in the snow/firn pack which were not done for the QIC (Brimblecombe et al., 1987; Cragin et al., 1993; Davies et al., 1982; Davis et al., 1995; Ginot et al., 2001; Hou and Qin, 2002; Li et al., 2006; Trachsel et al., 2019). The mobility of elements is not fixed in an equal sequence for every glacier; thus, it can vary depending on the concentration of the ion (Avak et al., 2019; Cragin et al., 1993) and the form that this ion is assuming in the glacier. For example, species that are in higher concentration can elute faster (Avak et al., 2018), and Cl^- in salts is much more stable than Cl^- in HCl form (Ginot et al., 2001). Cl^- has similar concentration values compared to Na^+; hence, we exclude concentration as the main reason why Cl^- elutes faster in some zones of the ice core.

https://doi.org/10.5194/egusphere-2026-4779
Preprint. Discussion started: 23 September 2026

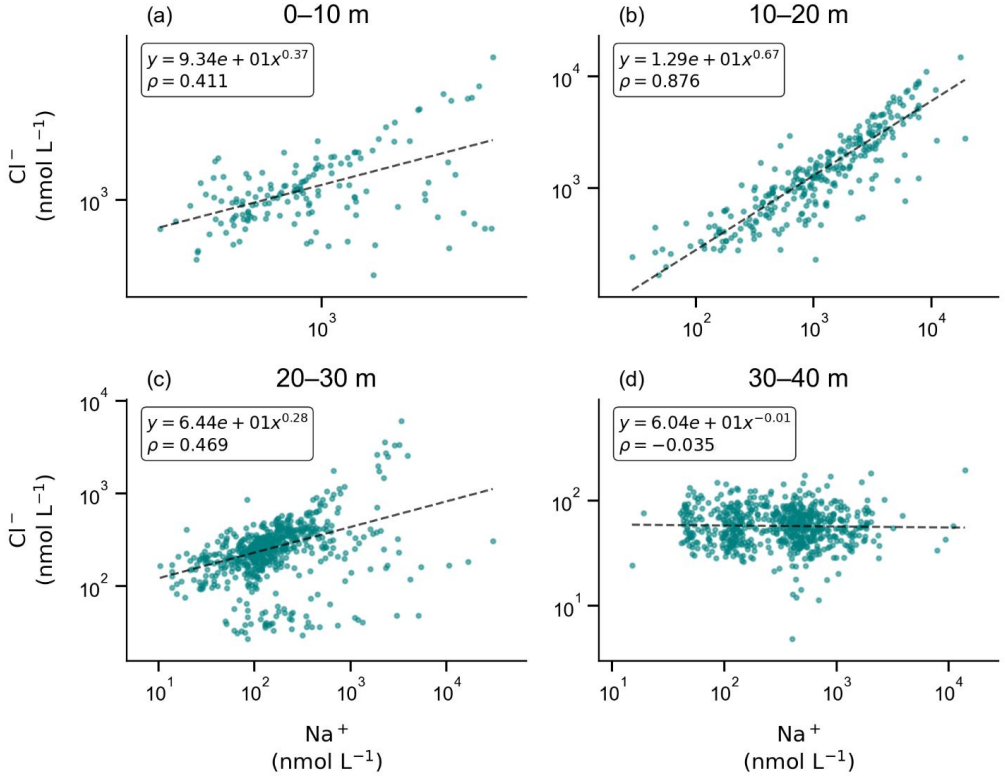

Figure 7: 10 m depth window Spearman correlation and robust log-log regression between Na^+ and Cl^-. In (a) correlation for depths between 0 and 10 m. In (b), depth window between 10 and 20 m. In (c), depth window between 20 and 30 m and in D, depth window between 30 to 40 m.

If concentration is not responsible for the preferential elution of Cl^-, the cation to which it is bonded might be. As previously stated, Cl^- is in general bonded to Na^+, however it can also bond to Mg^{2+}, Ca^{2+} and K^+. A log-log regression and Spearman correlation between Cl^- and the previously mentioned cations (Fig. S1, S2 and S3), however, indicates that the decoupling in depths between 30 and 40 meters also exists between Cl^- and these cations. It appears that at this depth Cl^- is not related to any of the major ions analyzed and it might be bonded to H^+. If that is the case, Na^+ must then be bonded to other anions, such as SO_4^{2-} and NO_3^-. Assessing the behavior of these anions in correlation with Na^+ using the same techniques as before (Figure 8) shows that Na^+ is weakly to very weakly correlated with them in the most superficial layers (from 0 to 10 m), where Cl^- is strongly correlated with Na^+. However, from 30 to 40 m depth, Na^+ becomes moderately correlated to SO_4^{2-} and NO_3^- ($\rho = 0.513$ and $\rho = 0.472$, respectively). This suggests that for some reason, at this depth interval, Na^+ bonds more to SO_4^{2-} and NO_3^- than to Cl^-. This is discussed in the next section.

https://doi.org/10.5194/egusphere-2026-4779
Preprint. Discussion started: 23 September 2026

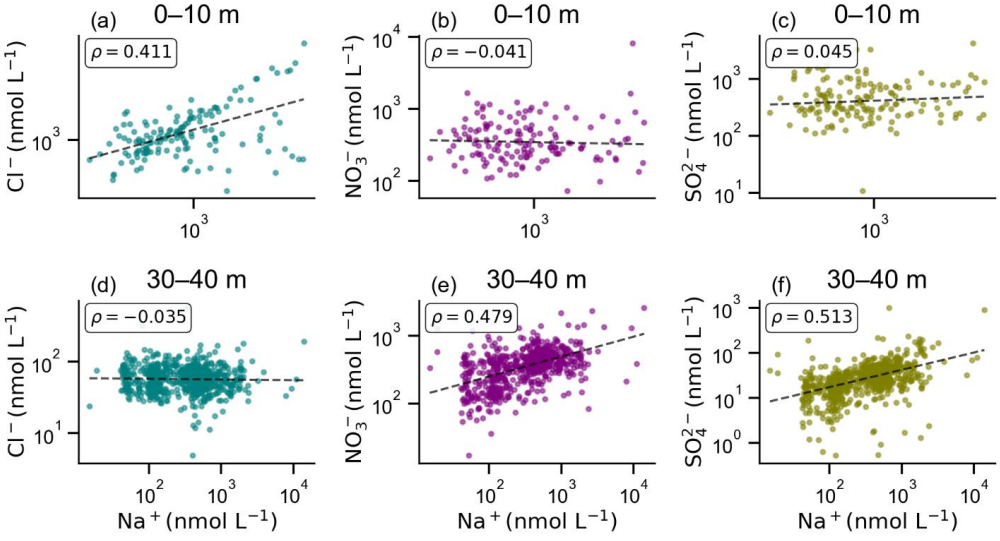

Figure 8: Log-log regression and Spearman correlation between Na^+ and Cl^-, NO_3^- and SO_4^{2-} for chosen depth intervals.

3.7 Acid-Mediated Ion Redistribution

The correlation between ions presented in the previous section suggests that ions undergo alterations that would force new combinations. In this section we propose a mechanism for why that may happen. As discussed before, the high concentrations of SO_4^{2-} in the first meters of the ice core indicate a possible mix of volcanic and anthropic sources. Sulfate is very weakly correlated to Na^+ at the surface, but it is moderately correlated with Ca^{2+}. Gypsum ($CaSO_4$) is a common component of local dust (Lindau et al., 2021). It could be that part of the sulfate might be deposited at the surface of the firn pack in gypsum particles, however, it is difficult to constrain whether gypsum is transported from the source areas and deposited as gypsum, or if it is formed by the reaction of calcium carbonate ($CaCO_3$) with H_2SO_4 in the atmosphere, as pointed out as a by Lindau (2021) for the Illimani ice core in Bolivia. The latter could happen in the QIC context considering the eruption phase of the Sabancaya volcano, discussed previously, that ejected high amounts of SO_2 into the atmosphere, which could form H_2SO_4 and promote the transformation of calcium carbonate into gypsum. Nitrate on the other hand is not highly concentrated at the surface of the firn pack, although it has some intense and sharp peaks marking individual strong deposition episodes. Nitrate is very weakly correlated with Na^+ and weakly correlated with Ca^{2+} at the surface layers of the firn pack. At the depth interval between 30 and 40 m, Cl^- correlation with Na^+ goes from moderate to very weak and the correlation between sulfate and nitrate with Na^+ goes from very weak to moderate (Figure 8). This behavior suggests a change in the preferential co-variation between ions right below the WT.

Sulfate and nitrate are commonly the first ions to be eluted, while Cl^- is one of the last, as described by Herreros et al. (2009), who studied the elution process in the Coropuna ice cap, close to the QIC, in southern Peru. The observed shift in the correlation behaviors suggests that, for this specific depth range, the mobilization of ions doesn't follow the standard elution sequence patterns. The relative increase in the association between Na^+ and sulfate and nitrate concomitant to the decoupling of Na-Cl correlation suggests that the mobility of ions is favoring the removal of Cl^-. It could be argued that

https://doi.org/10.5194/egusphere-2026-4779
Preprint. Discussion started: 23 September 2026

an early elution of nitrate and sulfate promotes acidification of the water within the WT. As this relatively more acidic water migrates down the ice column, it could facilitate ion exchange, alter mobility and enhance specific ion removal. If this were an extensive process, sulfate and nitrate would be expected to be attenuated above the chloride depletion zone and enriched within it. This is not observed. When calculating the ionic balance by subtracting major cations from major anions (Figure 9), we obtain the H^+ in excess, which indicates acidity. The more acidic zones of the ice core are right on top of the WT level (from around 15 to 18.99 m depth) and from around 25 to 40 m depth, in the chloride depletion zone. The depletion of chloride appears to be more pronounced than a possible redistribution of sulfate and nitrate, suggesting that the processes controlling this depletion may happen at a smaller spatial scale than can be resolved from bulk concentration profiles.

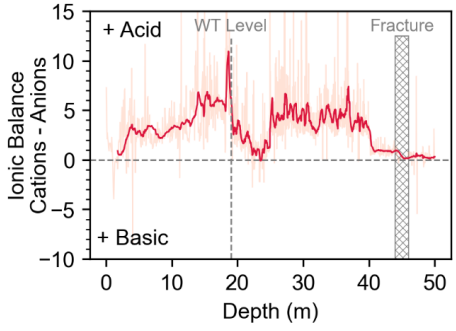

Figure 9: Ionic balance calculated using major ions.

3.8 PCA & Fuzzy C-Means Clustering (FCM)

The previous sections described and discussed the main interactions happening between ions and BC in the ice core. However, the extent of these alterations in depth is still uncertain. In this section, multivariate techniques are implemented to scan the ice core for similar chemical behavior. A PCA was calculated for depths between 0 and 45 m, the interval considered affected by the WT and the fracture and was then extrapolated to the entire ice core to evaluate a possible chemical melt signal in deeper depths. Three PCs were retained according to the Kaiser criterion (eigen values > 1) and the inspection of the scree plot, explaining 64.10 % of the total variance (Table 3). KMO test was higher than 0.6, and Bartlett's test of sphericity was below 0.01, confirming the suitability of the dataset to PCA calculation. Although the explained total variation leaves a substantial fraction of the dataset outside the retained components, the purpose of PCA is to reduce the dataset dimension for subsequent clustering and screening of the ice core rather than a complete reconstruction of the processes controlling chemical variance. The three retained components capture the dominant variance structure to feed the FCM analysis. The description of the chemical representation of each PC is given in Table 3 below. PC1 is dominated by Na^+, levoglucosan and K^+ with positive scores and MSA with negative score, PC2 by Mg^{2+}, Ca^{2+}, and NH_4^+, and PC3 by SO_4^{2-}, MSA, Cl^-, and Br^-. These components were not interpreted as representative of individual source processes, but rather as statistically distinct main chemical signatures composing the ice core that could be used for signal classification.

Table 3: Loadings of the chemical species for each PC kept for analysis.

Species	PC1	PC2	PC3
Explained Variance (%)	31.68	19.21	13.21

https://doi.org/10.5194/egusphere-2026-4779
Preprint. Discussion started: 23 September 2026

Cumulative Variance (%)	31.68	50.89	64.1
Na^+	**0.54**	-0.009	0.03
NH_4^+	0.20	**0.40**	-0.03
K^+	**0.43**	0.19	0.006
Mg^{2+}	-0.09	**0.64**	-0.01
Ca^{2+}	0.5	**0.55**	0.007
Cl^-	0.19	-0.01	**0.42**
NO_3^-	0.21	0.11	0.07
SO_4^{2-}	0.02	0.06	**0.60**
MSA	**-0.42**	0.10	**0.56**
Br^-	0.11	-0.14	**0.31**
Levoglucosan	**0.43**	-0.21	0.17

The results of the PCA were clustered using a Fuzzy C-Means Clustering (FCM) technique and each sample was assigned a degree of membership to the clusters (n = 3) that sum up to 1(Figure 10). Cluster 1 (C1) is characterized by negative values of PC1, PC2 fluctuating around zero, and varying (generally from +2.5 to −3) PC3 (Figure 10(a) and (b)). Hence, it is mainly represented by MSA and secondarily by Cl^-, SO_4^{2-}, MSA and Br^-. Cluster 2 (C2) is marked by varying PC1 (from +4 to −2), negative PC2, and positive PC3 (Figure 10(a) and (b)). It is characterized by SO_4^{2-}, MSA, Cl^-, and Br^- (from PC3) and variably by Na^+, K^+, levoglucosan (from positive PC1) and MSA (from negative PC1). Cluster 3 (C3) is characterized by negative PC1, PC2 and PC3 and it is thus composed of MSA. The FCM identified three clusters with distinct chemical signatures.

To assess the dominance of each cluster in depth, a membership depth profile was plotted (Figure 10(c)). In the first meters of ice core, right above WT, the dominant cluster is C2. Right where the WT level is observed, the dominance of C2 drops and a mixture of clusters takes place. From 25 m down to 40 m depth, C1 dominates. At around 40 m depth another mixing of clusters is observable. Below that depth, C3 dominates until 100 m depth, where yet another cluster mixing is seen. Below that, C2 dominates again.

https://doi.org/10.5194/egusphere-2026-4779
Preprint. Discussion started: 23 September 2026

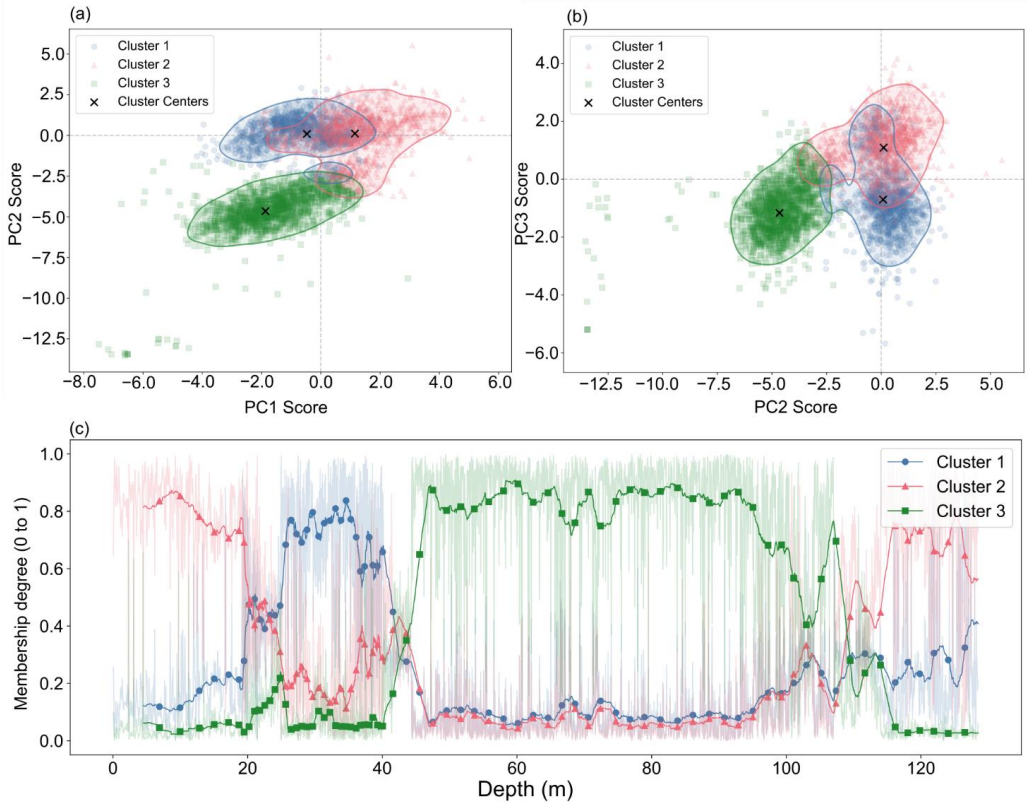

Figure 10: Panel (a) shows the Fuzzy C-Means (FCM) clusters in the Principal Component Analysis (PCA) space (Principal Component 1 (PC1) vs Principal Component 2 (PC2)). Panel (b) shows the FCM clusters in the PCA space (PC2 vs PC3). Cluster 1 is represented by blue dots and blue shaded areas; Cluster 2 is represented by red triangles and red shaded areas, and Cluster 3 is represented by green squares and green shaded areas. Panel (c) shows the membership degree of each sample to each cluster along the ice core depth.

Importantly, the highest membership of C1 occurs between 18 and 40 m depth, coinciding with the interval independently identified previously, by the assessment of concentration profiles, variance, SNR and the correlation analysis, as altered due to a combination of WT and fractured ice influence. It is considered a cluster that represents a zone with an altered signal. To constrain the zones with mixed clusterization, a depth profile of the cluster ambiguity is plotted (Figure 11). Scores closer to 1 are considered pure signal, while scores of 0.33 are considered the total ambiguity of the cluster, i.e., a mixture of cluster dominance and no clear chemical signature. The superficial firn pack not directly affected by the WT (from 0 to 18 m depth) shows scores around 0.75; it is thus considered a relatively pure signal composed of C2 in its majority and C1 (scores around 0.2) as a secondary factor (Figure 10(c)), suggesting a small fraction of altered signal. Right on the WT level, the membership scores drop and approach the ambiguity line, indicating a loss of statistically representative chemical signature. The ambiguity continues until 25 m depth, from where the cluster dominance becomes relatively pure again until 40 m depth. This depth range is not characterized by cluster ambiguity, but by the dominance of C1, indicating that despite being altered, this section maintains a chemical signature. It is difficult to constrain the exact WT thickness; however, it is possible to identify that the cluster ambiguity happens from approximately 19 down to 25 m, consistent with the extent of the Cl^-/Na^+ peak zone, which could reflect intense mixing processes potentially related to the presence of an aquifer. The dominance of C1 in the ice sections below that may reflect a region affected by the WT

https://doi.org/10.5194/egusphere-2026-4779
Preprint. Discussion started: 23 September 2026

in the recent past and/or by present water percolation through fractures. Close to the depths where the fracture was observed, another ambiguity zone is observed, after which the signal becomes relatively pure again, represented mostly by C3. The ambiguity close to the fracture is not the only characteristic that the fracture has in common with the WT. The acidity in the WT and close to the fracture is relatively more neutral than the section between 25 and 40 m depth, considered the altered section. Apart from that, a slight attenuation of the signal of some ions and a weak increase in the Cl^-/Na^+ ratio are also observed (Figure 3). Based on what was discussed until now, the fracture at 45 m depth could be filled with water and could also serve as a preferential drainage pathway. A third ambiguity zone is seen at depths between approximately 108 and 115 m. At these depths the sodium-chloride correlation presents a slight decline (from $\rho = 0.736$ to $\rho = 0.445$), the same behavior is seen, although more intensely, in the sodium-sulfate and sodium-nitrate systems ($\rho = 0.481$ to $\rho = -0.056$ and $\rho = 0.337$ to $\rho = -0.121$, respectively). The deep ice appears to have some mixing of signal that needs further discussion. Preliminary results as well as the results reported in (Clifford et al., 2023) indicate that the QIC's deep ice is likely highly compressed. It could then record more annual layers than previously thought. To better discuss this issue, ultra-high-resolution analyses (e.g. laser ablation) are being done. Having this in mind, we refrain from making assumptions on the state of the deep ice in this paper.

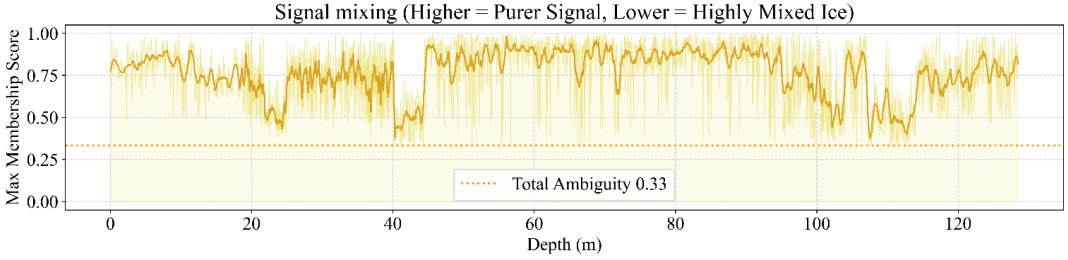

Figure 11: The signal mixing retrieved from the maximum membership score of each sample through depth along the ice core. The light-yellow represents the raw signal, while the dark yellow represents the smoothed (n=31 samples) signal. The orange dotted line represents total ambiguity, i.e. equal weight of cluster membership.

Overall, the PCA-FCM framework was able to independently identify the WT, the fracture zone and another, previously unknown, deep ice anomaly as intervals of enhanced signal mixing, which supports the interpretation that the chemical preservation varies significantly along the ice core.

4 Conclusions

In 2022, a new ice core was drilled at the Quelccaya Ice Cap, providing what may be one of the last opportunities to assess a high-resolution tropical paleoclimate archive before warming completelly erases the record. Given the scenario of intensified loss of glacial mass and the rise of the equilibrium line altitude worldwide, the risk of loss of glaciochemical signals, and, consequently, of paleoclimatological records, due to post-depositional alterations (e.g. melting, water percolation, photolysis etc.) is concerning. The study of tropical and temperate glaciers under these conditions is gaining importance (Avak et al., 2018, 2019; Herreros et al., 2009; Moser et al., 2024; Spagnesi et al., 2023; Watanabe et al.,

https://doi.org/10.5194/egusphere-2026-4779
Preprint. Discussion started: 23 September 2026

2015; Zhang and Kang, 2025). Locally, the effect that warming and melting can have on the chemical signal at QIC was already under discussion (Thompson et al., 2017, 2021) though it focused on water stable isotopes.

The analysis conducted in this work aims to evaluate and describe the chemical dynamics involved in a warming tropical ice cap ice core, identify alterations in the signal, and describe its preservation state. During the drilling of the ice core, we identified the presence of a water table that is related to the firn-ice transition, although its thickness remains uncertain. A major fracture was also identified below the water table, at 45 m depth.

Multiple independent tools, including concentration profiles, statistical indicators as well as multivariate analysis, allowed us to identify major behaviors of the chemical species, e.g. the accumulation and increased concentration of some ion species above the water table and the preserved signal of black carbon. Black carbon was considered a relatively stable parameter with seasonal variation that could be used to constrain the behavior of other species. The comparison between BC and soluble chemical species, plus the information retrieved from the statistical analysis revealed that Cl^- and SO_4^{2-} are the most affected ions by the post-depositional processes, however, they are affected differently and the alteration is depth-dependent. The ice section between the WT and the fracture is affected by a process that doesn't follow the standard elution sequence proposed for a glacier nearby (Herreros et al., 2009), with washout of Cl^- and the increased correlation between Na^+ and sulfate and nitrate. We propose that such differential alteration could be related to the acidification of the ice pack, which is supported by the ionic balance calculations made. The ice section below the fracture shows an attenuated signal, especially for SO_4^{2-}. Despite the dampening in intensity, the periodicity and the more intense peaks are still recognizable for most species in depth. The multivariate analysis helpes to constrain the altered regions and to identify other zones of concern in depth. One cluster (C1) was consistently associated with the chemically altered signal of the zone between the WT and the fracture. It occurs weakly as a secondary cluster in the superficial firn pack. A cluster ambiguity plot was used to identify the mixing of signals. This technique allowed the identification of highly mixed signals at the WT, near the fracture, and in the deep ice. A combination of evidence supports the hypothesis that the fracture could be filled with water and act as a preferential drainage pathway. Such evidence was not found for the signal in the deep ice, which is highly compressed; therefore, we refrain from making further assumptions as we identify the need for further investigation with ultra-high-resolution techniques (e.g., LA-ICP-MS).

This is one of the first publications in a series being prepared to study the Quelccaya ice core retrieved in 2022. Since the QIC is located in a zone that raises valid concerns regarding chemical preservation, we assessed and identified the extent of such alterations. We delimited the depths of higher mixing of signal and identified the depths with less alteration. Although melting and meltwater percolation are significant at the QIC, we demonstrated that soluble chemistry signal alteration is locally concentrated and associated with the WT and the fracture, rather than being uniformly distributed throughout the ice core

0–15 m: preserved signals for most ions, slightly smoothing of seasonal peaks.

15–20 m: preserved signal and intensification of concentration due to WT.

20–45 m: altered signal, loss of signal for some ions.

45–100 m: attenuation by diffusivity but preserved signal.

100–110 m: zone with disturbed signal, needs further investigation.

110–128.5 m: strongly-compressed ice, complex signal structure

https://doi.org/10.5194/egusphere-2026-4779
Preprint. Discussion started: 23 September 2026

This result is important for the subsequent work that will analyze the preserved signal for climatic discussions. Furthermore, the results show that sites under warming conditions could still preserve paleoclimatological records, but these records are facing an imminent threat. The 2022 QIC ice core might be the last chance to recover data from the Quelccaya Ice Cap, as mass loss in this place is very fast and predictions say the equilibrium line altitude might exceed the summit altitude as soon as 2050 (Yarleque et al., 2018). The analytical approach presented here may also prove useful for evaluating chemical preservation in other temperate and tropical glacier archives increasingly affected by meltwater percolation.

Code & Data Availability

The code used for the PCA-FCM data analysis is available from Zenodo at https://doi.org/10.5281/zenodo.21889387. The ice core dataset is archived in PANGAEA(Ilha et al., 2026). .

Author Contributions

JGI: Conceptualization, Methodology, Investigation, Resources, Data curation, Formal analysis, Software, Validation, Visualization, Writing – original draft, Writing – review & editing.

MBPP: Methodology, Investigation, Resources, Data curation, Software, Validation, Writing – review & editing.

OG: Methodology, Investigation, Resources, Project administration.

FL: Methodology, Investigation, Resources, Writing – review & editing, Project administration.

EB: Methodology, Investigation, Resources, Data curation, Formal analysis, Software, Validation, Writing – review & editing.

MP: Methodology, Investigation, Resources, Writing – review & editing, Project administration.

SK: Methodology, Investigation, Resources, Data curation, Software, Validation, Writing – review & editing, Supervision.

CB: Conceptualization, Methodology, Resources, Supervision, Project administration, Funding acquisition.

JS: Conceptualization, Methodology, Resources, Writing – review & editing, Supervision, Project administration, Funding acquisition.

PM: Conceptualization, Methodology, Investigation, Resources, Writing – review & editing, Supervision, Project administration, Funding acquisition.

Competing Interests

The authors have no competing interests.

Acknowledgments

The authors would like to thank the Cchuana family for all the logistical support during the field campaign, Elliot Moravec for the drill operation, Giovanni Baccolo, Andrea Spolaor and Pascal Bohleber for all the fruitful and very important

https://doi.org/10.5194/egusphere-2026-4779
Preprint. Discussion started: 23 September 2026

scientific discussions, Víctor Bustínza Urviola, Alexzander Santiago Martel, Rafael Santos dos Reis and Fernanda Luz for fieldwork and data acquisition support.

Financial Support

This research is a joint contribution between the Climate Change Institute, University of Maine, Orono, USA, with research funded by the US National Science Foundation P2C2 AGS-1600018, the Unidad de Glaciología y Recursos Hídricos, Universidad Nacional de San Antonio de Abad del Cusco (UNSAAC), the Autoridad Nacional de Agua and the Instituto Nacional de Investigación en Glaciares y Ecosistemas de Montaña (INAIGEM), Peru, the Centro Polar e Climático, Universidade Federal do Rio Grande do Sul (UFRGS), Porto Alegre, Brazil, and the Brazilian National Institute of Cryosphere Science and Technology, funded by the National Council for Scientific and Technological Development (CNPq), projects 465680/2014-3 and 422695/2021-1.The research also received additional funding support from the Ice Memory Project and the Follow the Ice Project.

References

Abdi, H. and Williams, L. J.: Principal component analysis, WIREs Computational Stats, 2, 433–459, https://doi.org/10.1002/wics.101, 2010.

Artaxo, P., Rizzo, L. V., Brito, J. F., Barbosa, H. M. J., Arana, A., Sena, E. T., Cirino, G. G., Bastos, W., Martin, S. T., and Andreae, M. O.: Atmospheric aerosols in Amazonia and land use change: from natural biogenic to biomass burning conditions, Faraday Discuss., 165, 203, https://doi.org/10.1039/c3fd00052d, 2013.

Avak, S. E., Schwikowski, M., and Eichler, A.: Impact and implications of meltwater percolation on trace element records observed in a high-Alpine ice core, J. Glaciol., 64, 877–886, https://doi.org/10.1017/jog.2018.74, 2018.

Avak, S. E., Trachsel, J. C., Edebeli, J., Brütsch, S., Bartels-Rausch, T., Schneebeli, M., Schwikowski, M., and Eichler, A.: Melt-Induced Fractionation of Major Ions and Trace Elements in an Alpine Snowpack, JGR Earth Surface, 124, 1647–1657, https://doi.org/10.1029/2019JF005026, 2019.

Baccolo, G., Eichler, A., Jenk, T. M., Burgay, F., and Schwikowski, M.: A review on ice cores from temperate glaciers: Processes, signal preservation and paleoclimatic significance, J. Glaciol., 72, e59, https://doi.org/10.1017/jog.2026.10182, 2026.

Barbaro, E., Padoan, S., Kirchgeorg, T., Zangrando, R., Toscano, G., Barbante, C., and Gambaro, A.: Particle size distribution of inorganic and organic ions in coastal and inland Antarctic aerosol, Environ Sci Pollut Res, 24, 2724–2733, https://doi.org/10.1007/s11356-016-8042-x, 2017.

Barbaro, E., Morabito, E., Gregoris, E., Feltracco, M., Gabrieli, J., Vardè, M., Cairns, W. R. L., Dallo, F., De Blasi, F., Zangrando, R., Barbante, C., and Gambaro, A.: Col Margherita Observatory: A background site in the Eastern Italian Alps for investigating the chemical composition of atmospheric aerosols, Atmospheric Environment, 221, 117071, https://doi.org/10.1016/j.atmosenv.2019.117071, 2020.

Beal, S. A., Kelly, M. A., Stroup, J. S., Jackson, B. P., Lowell, T. V., and Tapia, P. M.: Natural and anthropogenic variations in atmospheric mercury deposition during the Holocene near Quelccaya Ice Cap, Peru: Holocene Mercury Deposition, Global Biogeochem. Cycles, 28, 437–450, https://doi.org/10.1002/2013GB004780, 2014.

Bezdek, J. C.: Pattern Recognition with Fuzzy Objective Function Algorithms, Springer US, Boston, MA, https://doi.org/10.1007/978-1-4757-0450-1, 1981.

Bochang, Y. and Xuejing, X.: Fuzzy cluster analysis in geochemical exploration, Journal of Geochemical Exploration, 23, 281–291, https://doi.org/https://doi.org/10.1016/0375-6742(85)90031-7, 1985.

https://doi.org/10.5194/egusphere-2026-4779
Preprint. Discussion started: 23 September 2026

Bohleber, P., Stoll, N., Larkman, P., Rhodes, R. H., and Clases, D.: New evidence on the microstructural localization of sulfur and chlorine in polar ice cores with implications for impurity diffusion, The Cryosphere, 19, 5485–5498, https://doi.org/10.5194/tc-19-5485-2025, 2025.

Brimblecombe, P., Clegg, S. L., Davies, T. D., Shooter, D., and Tranter, M.: Observations of the preferential loss of major ions from melting snow and laboratory ice, Water Research, 21, 1279–1286, https://doi.org/10.1016/0043-1354(87)90181-3, 1987.

Buffen, A. M., Hastings, M. G., Thompson, L. G., and Mosley-Thompson, E.: Investigating the preservation of nitrate isotopic composition in a tropical ice core from the Quelccaya Ice Cap, Peru: NO3--N and -O isotopes in Quelccaya ice, J. Geophys. Res. Atmos., 119, 2674–2697, https://doi.org/10.1002/2013JD020715, 2014.

Clifford, H. M., Potocki, M., Rodda, C., Dixon, D., Birkel, S., Handley, M., Korotkikh, E., Introne, D., Schwanck, F., Tavares, F. A., Bernardo, R. T., Lindau, F. G. L., Gomez, O. V., Jara-Infantes, H., Urviola, V. B., Perry, L. B., Maurer, J., Seimon, A., Schwikowski, M., Casassa, G., Hou, S., Kurbatov, A. V., Miner, K. R., Simões, J. C., and Mayewski, P. A.: Prefacing unexplored archives from Central Andean surface-to-bedrock ice cores through a multifaceted investigation of regional firn and ice core glaciochemistry, J. Glaciol., 69, 693–707, https://doi.org/10.1017/jog.2022.91, 2023.

Coppola, D., Valade, S., Masias, P., Laiolo, M., Massimetti, F., Campus, A., Aguilar, R., Anccasi, R., Apaza, F., Ccallata, B., Cigolini, C., Cruz, L. F., Finizola, A., Gonzales, K., Macedo, O., Miranda, R., Ortega, M., Paxi, R., Taipe, E., and Valdivia, D.: Shallow magma convection evidenced by excess degassing and thermal radiation during the dome-forming Sabancaya eruption (2012–2020), Bull Volcanol, 84, 16, https://doi.org/10.1007/s00445-022-01523-1, 2022.

Cragin, J. H., Hewitt, A. D., and Colbeck, S. C.: Elution of Ions from Melting Snow. Chromatographic Versus Metamorphic Mechanisms, 1993.

Dansgaard, W., Johnsen, S. J., Møller, J., and Langway, C. C.: One Thousand Centuries of Climatic Record from Camp Century on the Greenland Ice Sheet, Science, 166, 377–381, https://doi.org/10.1126/science.166.3903.377, 1969.

Davies, T. D., Vincent, C. E., and Brimblecombe, P.: Preferential elution of strong acids from a Norwegian ice cap, Nature, 300, 161–163, https://doi.org/10.1038/300161a0, 1982.

Davis, R. E., Petersen, C. E., and Bales, R. C.: Ion flux through a shallow snowpack: effects of initial conditions and melt sequences, 1995.

Delmas, R. J., Ascencio, J.-M., and Legrand, M.: Polar ice evidence that atmospheric CO2 20,000 yr BP was 50% of present, Nature, 284, 155–157, https://doi.org/10.1038/284155a0, 1980.

Dunn, J. C.: A Fuzzy Relative of the ISODATA Process and Its Use in Detecting Compact Well-Separated Clusters, Journal of Cybernetics, 3, 32–57, https://doi.org/10.1080/01969727308546046, 1973.

Eichler, A., Schwikowski, M., and Gaggeler, H. W.: Meltwater-induced relocation of chemical species in Alpine firn, Tellus B, 53, 192–203, https://doi.org/10.1034/j.1600-0889.2001.d01-15.x, 2001.

EPICA community members: Eight glacial cycles from an Antarctic ice core, Nature, 429, 623–628, https://doi.org/10.1038/nature02599, 2004.

Epstein, S., Sharp, R. P., and Gow, A. J.: Antarctic Ice Sheet: Stable Isotope Analyses of Byrd Station Cores and Interhemispheric Climatic Implications, Science, 168, 1570–1572, https://doi.org/10.1126/science.168.3939.1570, 1970.

Fatehi, M. and Asadi, H. H.: Application of semi-supervised fuzzy c-means method in clustering multivariate geochemical data, a case study from the Dalli Cu-Au porphyry deposit in central Iran, Ore Geology Reviews, 81, 245–255, https://doi.org/https://doi.org/10.1016/j.oregeorev.2016.10.002, 2017.

Finlayson-Pitts, B. J. and Pitts Jr., J. N.: Chemistry of the upper and lower atmosphere: theory, experiments, and applications, Elsevier, 969 pp., 1999.

Fritz, S. C., Brinson, B. E., Billups, W. E., and Thompson, L. G.: Diatoms at >5000 Meters in the Quelccaya Summit Dome Glacier, Peru, Arctic, Antarctic, and Alpine Research, 47, 369–374, https://doi.org/10.1657/AAAR0014-075, 2015.

https://doi.org/10.5194/egusphere-2026-4779
Preprint. Discussion started: 23 September 2026

Gabrielli, P., Barbante, C., Bertagna, G., Bertó, M., Binder, D., Carton, A., Carturan, L., Cazorzi, F., Cozzi, G., Dalla Fontana, G., Davis, M., De Blasi, F., Dinale, R., Dragà, G., Dreossi, G., Festi, D., Frezzotti, M., Gabrieli, J., Galos, S. P., Ginot, P., Heidenwolf, P., Jenk, T. M., Kehrwald, N., Kenny, D., Magand, O., Mair, V., Mikhalenko, V., Lin, P. N., Oeggl, K., Piffer, G., Rinaldi, M., Schotterer, U., Schwikowski, M., Seppi, R., Spolaor, A., Stenni, B., Tonidandel, D., Uglietti, C., Zagorodnov, V., Zanoner, T., and Zennaro, P.: Age of the Mt. Ortles ice cores, the Tyrolean Iceman and glaciation of the highest summit of South Tyrol since the Northern Hemisphere Climatic Optimum, The Cryosphere, 10, 2779–2797, https://doi.org/10.5194/tc-10-2779-2016, 2016.

Gambaro, A., Zangrando, R., Gabrielli, P., Barbante, C., and Cescon, P.: Direct Determination of Levoglucosan at the Picogram per Milliliter Level in Antarctic Ice by High-Performance Liquid Chromatography/Electrospray Ionization Triple Quadrupole Mass Spectrometry, Anal. Chem., 80, 1649–1655, https://doi.org/10.1021/ac701655x, 2008.

Gilardoni, S., Di Mauro, B., and Bonasoni, P.: Black carbon, organic carbon, and mineral dust in South American tropical glaciers: A review, Global and Planetary Change, 213, 103837, https://doi.org/10.1016/j.gloplacha.2022.103837, 2022.

Ginot, P., Kull, C., Schwikowski, M., Schotterer, U., and Gäggeler, H. W.: Effects of postdepositional processes on snow composition of a subtropical glacier (Cerro Tapado, Chilean Andes), J. Geophys. Res., 106, 32375–32386, https://doi.org/10.1029/2000JD000071, 2001.

Herreros, J., Moreno, I., Taupin, J.-D., Ginot, P., Patris, N., De Angelis, M., Ledru, M.-P., Delachaux, F., and Schotterer, U.: Environmental records from temperate glacier ice on Nevado Coropuna saddle, southern Peru, Adv. Geosci., 22, 27–34, https://doi.org/10.5194/adgeo-22-27-2009, 2009.

Hou, S. and Qin, D.: The effect of postdepositional process on the chemical profiles of snow pits in the percolation zone, Cold Regions Science and Technology, 34, 111–116, https://doi.org/10.1016/S0165-232X(01)00065-9, 2002.

Hurley, J. V., Vuille, M., Hardy, D. R., Burns, S. J., and Thompson, L. G.: Cold air incursions, δ^{18}O variability, and monsoon dynamics associated with snow days at Quelccaya Ice Cap, Peru, J. Geophys. Res. Atmos., 120, 7467–7487, https://doi.org/10.1002/2015JD023323, 2015.

Hurley, J. V., Vuille, M., and Hardy, D. R.: On the Interpretation of the ENSO Signal Embedded in the Stable Isotopic Composition of Quelccaya Ice Cap, Peru, J. Geophys. Res. Atmos., 124, 131–145, https://doi.org/10.1029/2018JD029064, 2019.

Ilha, J. G.: Principal Component Analysis coupled to Fuzzy C-Means Clustering for the 2022 Quelccaya ice core data analysis (1.0), Zenodo [code], https://doi.org/10.5281/zenodo.21889387, 2026.

Ilha, J. G., Barbaro, E., Portella, M. B. P., Lindau, F. G. L., Potocki, M., Barbante, C., Simões, J. C., and Mayewski, P. A.: Chemical Composition of the 2022 Quelccaya Ice Core: Major Ions, MSA, Bromide, and Levoglucosan, 2026.

Jardine, K., Yañez-Serrano, A. M., Williams, J., Kunert, N., Jardine, A., Taylor, T., Abrell, L., Artaxo, P., Guenther, A., Hewitt, C. N., House, E., Florentino, A. P., Manzi, A., Higuchi, N., Kesselmeier, J., Behrendt, T., Veres, P. R., Derstroff, B., Fuentes, J. D., Martin, S. T., and Andreae, M. O.: Dimethyl sulfide in the Amazon rain forest, Global Biogeochemical Cycles, 29, 19–32, https://doi.org/10.1002/2014GB004969, 2015.

Jouzel, J., Merlivat, L., and Lorius, C.: Deuterium excess in an East Antarctic ice core suggests higher relative humidity at the oceanic surface during the last glacial maximum, Nature, 299, 688–691, https://doi.org/10.1038/299688a0, 1982.

Lamantia, K. A., Larocca, L. J., Thompson, L. G., and Mark, B. G.: El Niño enhances snow-line rise and ice loss on the Quelccaya Ice Cap, Peru, The Cryosphere, 18, 4633–4644, https://doi.org/10.5194/tc-18-4633-2024, 2024.

Legrand, M. and Mayewski, P.: Glaciochemistry of polar ice cores: A review, Reviews of Geophysics, 35, 219–243, https://doi.org/10.1029/96RG03527, 1997.

Legrand, M., Feniet-Saigne, C., Sattzman, E. S., Germain, C., Barkov, N. I., and Petrov, V. N.: Ice-core record of oceanic emissions of dimethylsulphide during the last climate cycle, Nature, 350, 144–146, https://doi.org/10.1038/350144a0, 1991.

Legrand, M., Vorobyev, M., Bokuchava, D., Kutuzov, S., Plach, A., Stohl, A., Khairedinova, A., Mikhalenko, V., Vinogradova, M., Eckhardt, S., and Preunkert, S.: Measurement Report: Changes in ammonia emissions since the 18th

https://doi.org/10.5194/egusphere-2026-4779
Preprint. Discussion started: 23 September 2026

century in south-eastern Europe inferred from an Elbrus (Caucasus, Russia) ice-core record, Atmos. Chem. Phys., 25, 1385–1399, https://doi.org/10.5194/acp-25-1385-2025, 2025.

Li, Z., Edwards, R., Mosley-Thompson, E., Wang, F., Dong, Z., You, X., Li, H., Li, C., and Zhu, Y.: Seasonal variability of ionic concentrations in surface snow and elution processes in snow–firn packs at the PGPI site on Ürümqi glacier No. 1, eastern Tien Shan, China, Ann. Glaciol., 43, 250–256, https://doi.org/10.3189/172756406781812069, 2006.

Lindau, F. G. L., Simões, J. C., Delmonte, B., Ginot, P., Baccolo, G., Paleari, C. I., Di Stefano, E., Korotkikh, E., Introne, D. S., Maggi, V., Garzanti, E., and Andò, S.: Giant dust particles at Nevado Illimani: a proxy of summertime deep convection over the Bolivian Altiplano, The Cryosphere, 15, 1383–1397, https://doi.org/10.5194/tc-15-1383-2021, 2021.

Liu, J., Zhang, T., Ding, X., Li, X., Liu, Y., Yan, C., Shen, Y., Yao, X., and Zheng, M.: A clear north-to-south spatial gradience of chloride in marine aerosol in Chinese seas under the influence of East Asian Winter Monsoon, Science of The Total Environment, 832, 154929, https://doi.org/10.1016/j.scitotenv.2022.154929, 2022.

Marquetto, L., Kaspari, S., and Cardia Simões, J.: Refractory black carbon (rBC) variability in a 47-year West Antarctic snow and firn core, The Cryosphere, 14, 1537–1554, https://doi.org/10.5194/tc-14-1537-2020, 2020.

Mayewski, P. A., Lyons, W. B., Spencer, M. J., Twickler, M. S., Buck, C. F., and Whitlow, S.: An ice-core record of atmospheric response to anthropogenic sulphate and nitrate, Nature, 346, 554–556, https://doi.org/10.1038/346554a0, 1990.

Meng, H.-D., Song, Y.-C., Song, F.-Y., and Shen, H.-T.: Research and application of cluster and association analysis in geochemical data processing, Comput Geosci, 15, 87–98, https://doi.org/10.1007/s10596-010-9199-x, 2011.

Moser, D. E., Thomas, E. R., Nehrbass-Ahles, C., Eichler, A., and Wolff, E.: Review article: Melt-affected ice cores for polar research in a warming world, The Cryosphere, 18, 2691–2718, https://doi.org/10.5194/tc-18-2691-2024, 2024.

Osmont, D., Sigl, M., Eichler, A., Jenk, T. M., and Schwikowski, M.: A Holocene black carbon ice-core record of biomass burning in the Amazon Basin from Illimani, Bolivia, Clim. Past, 15, 579–592, https://doi.org/10.5194/cp-15-579-2019, 2019.

Osterberg, E. C., Handley, M. J., Sneed, S. B., Mayewski, P. A., and Kreutz, K. J.: Continuous Ice Core Melter System with Discrete Sampling for Major Ion, Trace Element, and Stable Isotope Analyses, Environ. Sci. Technol., 40, 3355–3361, https://doi.org/10.1021/es052536w, 2006.

Pfeiffer, M., Latorre, C., Gayo, E., and Amundson, R.: Rare calcium chloride–rich soil and implications for the existence of liquid water in a hyperarid environment, Geology, 47, 163–166, https://doi.org/10.1130/G45642.1, 2019.

Pueyo, J., Demergasso, C., Escudero, L., Chong, G., Cortéz-Rivera, P., Sanjurjo-Sánchez, J., Carmona, V., and Giralt, S.: On the origin of saline compounds in acidic salt flats (Central Andean Altiplano), Chemical Geology, 574, 120155, https://doi.org/10.1016/j.chemgeo.2021.120155, 2021.

Ramsay, R., Di Marco, C. F., Sörgel, M., Heal, M. R., Carbone, S., Artaxo, P., De Araùjo, A. C., Sá, M., Pöhlker, C., Lavric, J., Andreae, M. O., and Nemitz, E.: Concentrations and biosphere–atmosphere fluxes of inorganic trace gases and associated ionic aerosol counterparts over the Amazon rainforest, Atmos. Chem. Phys., 20, 15551–15584, https://doi.org/10.5194/acp-20-15551-2020, 2020.

Rempel, A. W., Waddington, E. D., Wettlaufer, J. S., and Worster, M. G.: Possible displacement of the climate signal in ancient ice by premelting and anomalous diffusion, Nature, 411, 568–571, https://doi.org/10.1038/35079043, 2001.

Ringnér, M.: What is principal component analysis?, Nat Biotechnol, 26, 303–304, https://doi.org/10.1038/nbt0308-303, 2008.

Salzmann, N., Huggel, C., Rohrer, M., Silverio, W., Mark, B. G., Burns, P., and Portocarrero, C.: Glacier changes and climate trends derived from multiple sources in the data scarce Cordillera Vilcanota region, southern Peruvian Andes, The Cryosphere, 7, 103–118, https://doi.org/10.5194/tc-7-103-2013, 2013.

Schwikowski, M., Brütsch, S., Gäggeler, H. W., and Schotterer, U.: A high-resolution air chemistry record from an Alpine ice core: Fiescherhorn glacier, Swiss Alps, J. Geophys. Res., 104, 13709–13719, https://doi.org/10.1029/1998JD100112, 1999.

https://doi.org/10.5194/egusphere-2026-4779
Preprint. Discussion started: 23 September 2026

Shlens, J.: A Tutorial on Principal Component Analysis, 2014.

Spagnesi, A., Bohleber, P., Barbaro, E., Feltracco, M., De Blasi, F., Dreossi, G., Stocker-Waldhuber, M., Festi, D., Gabrieli, J., Gambaro, A., Fischer, A., and Barbante, C.: Preservation of chemical and isotopic signatures within the Weißseespitze millennial old ice cap (Eastern Alps), despite the ongoing ice loss, Front. Earth Sci., 11, 1322411, https://doi.org/10.3389/feart.2023.1322411, 2023.

Spagnesi, A., Wachs, D., Bohleber, P., Barbaro, E., Feltracco, M., Festi, D., Oeggl, K., Gabrieli, J., Aeschbach, W., Oberthaler, M., Stocker-Waldhuber, M., Gambaro, A., Barbante, C., and Fischer, A.: New chemical signatures from Weißseespitze ice cores (Eastern Alps): pre-industrial pollution traces from Roman Empire to early modern period, Front. Earth Sci., 14, 1680019, https://doi.org/10.3389/feart.2026.1680019, 2026.

Stoll, N., Eichler, J., Hörhold, M., Shigeyama, W., and Weikusat, I.: A Review of the Microstructural Location of Impurities in Polar Ice and Their Impacts on Deformation, Front. Earth Sci., 8, 615613, https://doi.org/10.3389/feart.2020.615613, 2021.

Thompson, L. G. and Davis, M. E.: An 1800-year Ice Core History of Climate and Environment in the Andes of Southern Peru and its Relationship with Highland/Lowland Cultural Oscillations, 8, 2014.

Thompson, L. G. and Mosley-Thompson, E.: Evidence of Abrupt Climatic Change During the Last 1,500 Years Recorded in Ice Cores from the Tropical Quelccaya Ice Cap, Peru, in: Abrupt Climatic Change, edited by: Berger, W. H. and Labeyrie, L. D., Springer Netherlands, Dordrecht, 99–110, https://doi.org/10.1007/978-94-009-3993-6_9, 1987.

Thompson, L. G., Mosley-Thompson, E., and Arnao, B. M.: El Niño-Southern Oscillation Events Recorded in the Stratigraphy of the Tropical Quelccaya Ice Cap, Peru, Science, New Series, 226, 50–53, 1984a.

Thompson, L. G., Mosley-Thompson, E., Grootes, P. M., Pourchet, M., and Hastenrath, S.: Tropical glaciers: Potential for ice core paleoclimatic reconstructions, J. Geophys. Res., 89, 4638–4646, https://doi.org/10.1029/JD089iD03p04638, 1984b.

Thompson, L. G., Mosley-Thompson, E., Bolzan, J. F., and Koci, B. R.: A 1500-Year Record of Tropical Precipitation in Ice Cores from the Quelccaya Ice Cap, Peru, Science, 229, 971–973, https://doi.org/10.1126/science.229.4717.971, 1985.

Thompson, L. G., Mosley-Thompson, E., Dansgaard, W., and Grootes, P. M.: The Little Ice Age as Recorded in the Stratigraphy of the Tropical Quelccaya Ice Cap, Science, 234, 361–364, https://doi.org/10.1126/science.234.4774.361, 1986.

Thompson, L. G., Mosley-Thompson, E., Davis, M. E., and Brecher, H. H.: Tropical glaciers, recorders and indicators of climate change, are disappearing globally, Ann. Glaciol., 52, 23–34, https://doi.org/10.3189/172756411799096231, 2011.

Thompson, L. G., Mosley-Thompson, E., Davis, M. E., Zagorodnov, V. S., Howat, I. M., Mikhalenko, V. N., and Lin, P.-N.: Annually Resolved Ice Core Records of Tropical Climate Variability over the Past ~1800 Years, Science, 340, 945–950, https://doi.org/10.1126/science.1234210, 2013.

Thompson, L. G., Davis, M. E., Mosley-Thompson, E., Beaudon, E., Porter, S. E., Kutuzov, S., Lin, P. -N., Mikhalenko, V. N., and Mountain, K. R.: Impacts of Recent Warming and the 2015/2016 El Niño on Tropical Peruvian Ice Fields, J. Geophys. Res. Atmos., 122, https://doi.org/10.1002/2017JD026592, 2017.

Thompson, L. G., Davis, M. E., Mosley-Thompson, E., Porter, S. E., Corrales, G. V., Shuman, C. A., and Tucker, C. J.: The impacts of warming on rapidly retreating high-altitude, low-latitude glaciers and ice core-derived climate records, Global and Planetary Change, 203, 103538, https://doi.org/10.1016/j.gloplacha.2021.103538, 2021.

Trachsel, J. C., Avak, S. E., Edebeli, J., Schneebeli, M., Bartels-Rausch, T., Bruetsch, S., and Eichler, A.: Microscale Rearrangement of Ammonium Induced by Snow Metamorphism, Front. Earth Sci., 7, 194, https://doi.org/10.3389/feart.2019.00194, 2019.

Uglietti, C., Gabrielli, P., Cooke, C. A., Vallelonga, P., and Thompson, L. G.: Widespread pollution of the South American atmosphere predates the industrial revolution by 240 y, Proc. Natl. Acad. Sci. U.S.A., 112, 2349–2354, https://doi.org/10.1073/pnas.1421119112, 2015.

https://doi.org/10.5194/egusphere-2026-4779
Preprint. Discussion started: 23 September 2026

Verdin, K. L.: Digital Elevation Model (DEM) from the Hydrologic Derivatives for Modeling and Analysis (HDMA) database -- South America, https://doi.org/https://doi.org/10.5066/F7S180ZP, 2017.

Vimeux, F., Ginot, P., Schwikowski, M., Vuille, M., Hoffmann, G., Thompson, L. G., and Schotterer, U.: Climate variability during the last 1000 years inferred from Andean ice cores: A review of methodology and recent results, Palaeogeography, Palaeoclimatology, Palaeoecology, 281, 229–241, https://doi.org/10.1016/j.palaeo.2008.03.054, 2009.

Vriend, S. P., Gaans, P. F. M. van, Middelburg, J., and Nijs, A. de: The application of fuzzy c-means cluster analysis and non-linear mapping to geochemical datasets: examples from Portugal, Applied Geochemistry, 3, 213–224, https://doi.org/https://doi.org/10.1016/0883-2927(88)90009-1, 1988.

Vuille, M., Bradley, R. S., Healy, R., Werner, M., Hardy, D. R., Thompson, L. G., and Keimig, F.: Modeling δ18O in precipitation over the tropical Americas: 2. Simulation of the stable isotope signal in Andean ice cores, Journal of Geophysical Research: Atmospheres, 108, https://doi.org/10.1029/2001JD002039, 2003.

Vuille, M., Francou, B., Wagnon, P., Juen, I., Kaser, G., Mark, B. G., and Bradley, R. S.: Climate change and tropical Andean glaciers: Past, present and future, Earth-Science Reviews, 89, 79–96, https://doi.org/10.1016/j.earscirev.2008.04.002, 2008.

Watanabe, K., Hirai, T., and Kawada, K.: Ratios of Mg^{2+}/Na^{+} in the snow cover at Murododaira, Mt. Tateyama, Japan: On the possibility of an indicator of chemical leaching, Bulletin of Glacier Research, 33, 1–5, https://doi.org/10.5331/bgr.33.1, 2015.

Weide, D. M., Fritz, S. C., Brinson, B. E., Thompson, L. G., and Billups, W. E.: Freshwater diatoms in the Sajama, Quelccaya, and Coropuna glaciers of the South American Andes, Diatom Research, 32, 153–162, https://doi.org/10.1080/0269249X.2017.1335240, 2017.

Wendl, I. A., Menking, J. A., Färber, R., Gysel, M., Kaspari, S. D., Laborde, M. J. G., and Schwikowski, M.: Optimized method for black carbon analysis in ice and snow using the Single Particle Soot Photometer, Atmos. Meas. Tech., 7, 2667–2681, https://doi.org/10.5194/amt-7-2667-2014, 2014.

Wolff, E. W., Rankin, A. M., and Röthlisberger, R.: An ice core indicator of Antarctic sea ice production?, Geophysical Research Letters, 30, 2003GL018454, https://doi.org/10.1029/2003GL018454, 2003.

Xu, G., Gao, Y., Lin, Q., Li, W., and Chen, L.: Characteristics of water-soluble inorganic and organic ions in aerosols over the Southern Ocean and coastal East Antarctica during austral summer, JGR Atmospheres, 118, https://doi.org/10.1002/2013JD019496, 2013.

Xu, J., Hou, S., Chen, F., Ren, J., and Qin, D.: Tracing the sources of particles in the East Rongbuk ice core from Mt. Qomolangma, Sci. Bull., 54, 1781–1785, https://doi.org/10.1007/s11434-009-0050-5, 2009.

Yarleque, C., Vuille, M., Hardy, D. R., Timm, O. E., De la Cruz, J., Ramos, H., and Rabatel, A.: Projections of the future disappearance of the Quelccaya Ice Cap in the Central Andes, Sci Rep, 8, 15564, https://doi.org/10.1038/s41598-018-33698-z, 2018.

Zennaro, P., Kehrwald, N., McConnell, J. R., Schüpbach, S., Maselli, O. J., Marlon, J., Vallelonga, P., Leuenberger, D., Zangrando, R., Spolaor, A., Borrotti, M., Barbaro, E., Gambaro, A., and Barbante, C.: Fire in ice: two millennia of boreal forest fire history from the Greenland NEEM ice core, Clim. Past, 10, 1905–1924, https://doi.org/10.5194/cp-10-1905-2014, 2014.

Zennaro, P., Kehrwald, N., Marlon, J., Ruddiman, W. F., Brücher, T., Agostinelli, C., Dahl-Jensen, D., Zangrando, R., Gambaro, A., and Barbante, C.: Europe on fire three thousand years ago: Arson or climate?: HOLOCENE FIRE ACTIVITY IN THE NEEM CORE, Geophys. Res. Lett., 42, 5023–2033, https://doi.org/10.1002/2015GL064259, 2015.

Zhang, Y. and Kang, S.: Ice core evidence of rapid climate and environmental changes on the Tibetan plateau, Atmospheric Environment, 361, 121483, https://doi.org/10.1016/j.atmosenv.2025.121483, 2025.

Global Volcanism Program | Sabancaya, https://volcano.si.edu/volcano.cfm?vn=354006, last access: 27 July 2026, 2026., 2026.